Chapter 3

Antenna array maintenance using time domain reflectometry

The cable, balun and antenna that connect to the transmitter and/or receiver are important parts of the complete radar system. It is useful to know whether or not any of these components are operating outside their specification. The total failure of a component within this system may result in not obtaining the data required, while some component problems will, at the very least, adversely affect the time series collected. For instance, electrical discontinuities along a length of cable can affect the amplitude and phase recorded. Time Domain Reflectometry (TDR) is one technique available for probing the current characteristics of this important radar sub-system. The TDR technique involves sending a pulse through the coaxial cable and balun system, then observing the returned pulse. Changes in the form of the returned pulse are a result of the system it has travelled through. Unexpected variations in the returned pulse can reveal a range of information about the type of problem along the cable as well as its location.

While TDR can be a powerful tool in locating problems, other, more straightforward tools can be used to monitor equipment behaviour. For instance, establishing complex impedance behaviour at selected points along the cable, balun and antenna sub-system using a Vector Impedance Meter (VIM) is a simple but effective diagnostic

tool for general antenna array monitoring, with any deviations from expected value ranges indicating the possibility of existing or developing faults. Both TDR and VIM are two tools among others used for data collection in this study.

This Chapter describes a survey of the present state of the MF antenna array and summarises the problems faced and rectified in order to raise its operational capability. Areas discussed include the motivation for the current work, the equipment systems used in raw data collection via TDR, VIM and other techniques. Specific discussions on coaxial cable velocity factor and risetime are also mentioned in relation to their bearing on the reduction of the raw data and on the capability of the equipment systems used. An analysis of the reduced data is presented together with recommendations for continuing array management and possible areas of future work to maintain the antenna array's operational status. The conclusions drawn may be applicable to similar ageing arrays.

3.1 Introduction

As mentioned previously, an isolated region of the MF antenna array was struck by lightning on 12 January 1998. This caused minor damage to the antenna array but more severe damage to the connected receiving system, rendering data collection temporarily impossible. This break in near continuous MF radar observation from the site provided a unique opportunity for an investigation into the current state of the antenna array. Aims of this survey were to:

- Establish if any antenna array faults are present, their type and location.
- Repair all faults (based primarily on antenna priority) with the aim of the complete MF antenna array to be operational.
- Re-establish and re-organize the cable, balun and antenna maintenance database for efficient fault tracking.
- Establish the effectiveness of previous upgrades (i.e. *Vandepeer* [1993]).

- Establish effective techniques for regular array maintenance.
- Anticipate likely future maintenance problem areas and their solutions.

The objectives of the survey were to be completed as the MF radar transmitter and receiver system was re-commissioned following the repair of the RDAS by the manufacturer and subsequent complete system refurbishment by the Atmospheric Group detailed in section 2.3. This limited time period for significant continuous antenna array maintenance work was the first such period available since the antenna array upgrade of 1992 through 1994 due to the near continual operation of the complete radar system. Such an opportunity allowed marked progress in servicing commonly used antennas as well as increasing the operational status of under utilised ones. In fact it was envisaged that upon system re-commissioning, the third transmitter chassis would be integrated into the standard MF radar system. If used as designed (see *Vandepeer* [1993]) this system would require all 89 like polarised antennas from the array to be operational for transmission purposes[1]. This antenna requirement is a dramatic increase in demand for operational antennas compared to previous utilisation of the antenna array. This requirement was a primary motivation for the array survey outlined here as was the prospect of developing a more effective array management and maintenance programme for future implementation. The study detailed here was organised and managed by the author and completed with the substantial assistance of the technical staff.

Faults in the Cable-Balun-Antenna (CBA) sub-system are traditionally identified via five ways. First, the radar system attempts to self-calibrate the phase of each of its channels. During this *phase zero* cycle, which is initiated periodically (e.g. at the beginning of a multiple acquisition block), a RF signal from within each channel's Filter/TR switch is sampled. This channel sample enables each individual drive signal

[1]Note that to achieve this configuration, two dipoles need to be connected to one Filter/TR switch as opposed to the three dipoles to one Filter/TR switch connection provided by either of the two antenna patchboards. A solution to this requirement may involve the 2:1 splitter/combiner design outlined in Chapter 4.

to a PA module to be adjusted such that the signals at all Filter/TR switch outputs are in phase relative to each other. The number of phase steps required to achieve this state is recorded for each channel in the header of the acquired data file. Because the sampled signal within the Filter/TR switch is partly dependent on the load impedance of the antenna, any unusual variations in the recorded steps required for a successful *phase zero* cycle or the fact that a particular channel may not be able to attain a *phase zero* setting in this cycle may indicate a CBA sub-system fault, assuming all other possible causes have been eliminated.

Secondly, the output load impedance of the PA module is monitored throughout acquisition for abnormal reflected power. If the output load impedance exceeds 2:1 with respect to 50 Ω $\angle 0°$, the PA module will be shut down (indicated by a fault LED being tripped on that PA module). Because this output impedance can be affected by significant antenna impedance variations, a fault on a PA module can mean a CBA fault of some kind. Facility for this fault status to be logged is available but not implemented at the current time so only a visual clue is provided.

Thirdly, at the start of any observation period, the relative system phase errors are calculated (see section 6.3.1). This provides an estimate of phase behaviour inherent in each CBA sub-system used for reception relative to a reference CBA sub-system at that time. The accepted system phase errors are within certain limits and are relatively stable over time, with any change in sign or significant change in magnitude possibly indicating a fault in the respective CBA sub-system. Also, a visual inspection of individual time series may reveal abnormal noise structure or overall low level signal strength when compared to other receivers. The cause of these symptoms may be attributed to faults within a connected CBA sub-system.

Fourth, periodic sampling of the complex impedance at each antenna patchboard connection using a vector impedance meter identifies any CBA sub-system presenting a load departing from the nominal value of $\sim$75 Ω $\angle 0°$. Significant departures from the nominal values, in terms of magnitude and/or phase, can indicate CBA faults.

Finally, periodic visual inspection of the array can identify *downed* or *grounded* antennas as well as other mechanical malfunctions (i.e. broken dipole feeders or dipole insulators etc.) which may or may not be indicated by any of the preceding tests.

While a multi-facet approach to CBA fault finding such as that described above increases the likelihood of identifying many of the faults present, each individual approach has inherent limitations. For instance the lack of a channel successfully completing a phase zero cycle may indicate problems other than CBA sub-system faults. For the phase zero cycle to accurately and consistently indicate CBA sub-system faults, the Phase Control module and Filter/TR switch must be free from internal defects. Problems with the PC modules have been documented previously (see section 2.3.1.1, 2.3.2 and *Woithe & Grant* [1999]) whereas the Filter/TR switch, for example, may suffer from a de-tuned filter or other ailment. The continual operation of the MF radar system can lead to the development of faults in these transmitter chassis modules, at least in terms of natural component attrition, which may appear symptomatic of CBA sub-system faults. In a similar fashion the PA module output load SWR variation may be caused by problems within any component preceding the PA module. The detection and elimination of all faults internal to the transmitter chassis will allow more accurate CBA sub-system fault diagnosis if these multiple indicators are to be best utilised.

The use of atmospheric phase error values has significant pertinence to determining CBA faults because the values are obtained utilising a significant proportion of CBA hardware compared to the first two examples outlined above. In the first two examples, variations external to the CBA system can affect the evidence for a fault, whereas the atmospheric phase error values are mostly influenced by the CBA sub-system and the receiver channel of the RDAS. The receiver channel component exhibits a consistent quantifiable behaviour, resulting in the CBA sub-system's variation dominating any fluctuating behaviour of this combined hardware set. However, the application of atmospheric system phase error values to CBA fault finding in this survey highlights that unless the technique is applied carefully, the results may be inconclusive. While

they are suggestive of possible origins of faults when analysed (see section 3.3.3), there are inherent difficulties in their interpretation due to a) the temporal variations of each cable, balun and antenna system attached to the receiver as well as b) the completeness and currency of the data set use for such an analysis.

The visual inspection of individual time series for telltale signs of system hardware irregularities occurs sporadically considering most raw data files (containing individual receiver time series) are reduced to smaller *parameter* data files in routine operation. This means, for example, that noisy CBA sub-systems are often only identified when parameters of the reduced data fail to accurately describe normal atmospheric states or are nonsensical.

Similarly, the manual monitoring of antenna complex impedance and antenna array visual inspection has been irregular at best since the 1992/94 array upgrade. This allows the accumulation of faults to significant levels over a period of time to go unnoticed. Dealing with a large number of individual faults requires significant radar down-time, which is undesirable in most modern remote sensing applications.

Once CBA sub-systems have been identified as containing a fault, a more focused investigation can be carried out. Typically this involves a visual inspection of the CBA sub-system, with the use of vector impedance metering on selected components and sometimes TDR techniques. TDR is a technique that has the ability to focus on the CBA system alone. This addresses the problem indicated above that most current methods use indicators outside the CBA system to indicate problems *within* the CBA system. It was with this in mind that TDR techniques were included from the outset in the current antenna array survey.

TDR had been used during the installation of the array [*Rossiter*, 1970], subsequently for cable length and attenuation determinations [*Briggs*, 1977] and during an upgrade to the cable system for fault diagnosis of cable runs [*Vandepeer*, 1993]. In recent years TDR has been used intermittently for confirmation of cable faults and for a trial study of cable length and attenuation characteristics [*Holdsworth & Rutherford*,

1996, private communication] using a commercial TDR system[2].

The aforementioned work in this area has identified a number of problems indicative of the array, with the most significant being the containment of water inside the air-cored dielectric of the underground section of cable. In order to address all current problems encountered within the array it was envisaged that a strategy involving the use and development of previous techniques, combined with acquisition of new equipment such as a cable locator, could be used to restore the array to full operational status. Central to this strategy was the use and development of TDR equipment and techniques, which are outlined in the following sections.

3.2 TDR equipment and configuration

Time domain reflectometry of coaxial cable can be viewed as RADAR operation in a closed circuit. In this case, the closed circuit consists of a transmission line. Essentially, an electromagnetic pulse is directed through a medium and if a target in the medium is detected then at the very least range information can be determined. Further examination of the returned pulse may yield much more information about the target's and medium's characteristics. In our case the medium is a specific type of transmission line, the coaxial cable, and the target is any local discontinuity. However, other types of medium such as twisted pair and optical fibre can be substituted as well as completely different mediums such as digital electronics [*Bethke & Seifert*, 2001], polar liquids [*Cole*, 1977] or soil profiles [*Topp et al.*, 1980; *Dalton et al.*, 1984].

Time domain reflectometry may be accomplished via two main techniques, Step-Voltage TDR and Pulse/Impulse TDR (e.g. *Strickland et al.* [1970];*Matick* [1969];*Davidson* [1978]). Step-Voltage TDR uses a fast risetime, DC step to interrogate the transmission line. Here the pulse width is at least twice the delay time of the transmission line, with returns algebraically adding to the initial step voltage. As observed in *Editorial* [1974], the Step-Voltage technique retains the phase relationship between the

[2]The Tektronix 1503C Metallic Time Domain Reflectometer.

incident and reflected signal such that the absolute impedance and nature of the discontinuity can be resolved. Limitations of this technique are that narrow-band or frequency selective transmission lines cannot be reliably tested because the step requires a broad bandwidth to be transmitted. Alternatively, Pulse TDR uses a pulsed RF signal. This differs from Step-Voltage TDR in that the phase relationship between the incident and reflected pulse is lost due to the relatively small pulse width used compared to the electrical length of the transmission line under test and the non-overlap of incident and reflected pulses. Further shortening the pulse width requires an ever wider transmission line bandwidth and thus sets a theoretical limit on the resolution of the system, although in many practical TDR systems there are other factors that have a more immediate effect on the resolution obtained. The Pulse TDR technique will be described here because of its extensive use in the current maintenance programme. The applicability of the Pulse TDR technique to long transmission lines and no current requirement for detailed cable impedance measurements along a cable section dictated selection of this more appropriate technique.

In order to relate an electrical response to a mechanical configuration, when a pulse is sent down a transmission line, the distance (D) to a discontinuity is given by:

$$D = \frac{c}{\sqrt{\epsilon}} \frac{t}{2} \tag{3.1}$$

where c is the speed of light (metres per second), ϵ is the relative dielectric constant of the transmission system and t is the elapsed time between the input pulse and the reflected pulse (seconds).

Discontinuities are typically caused by any characteristic impedance (Z_O) variations along the transmission line. They can range from small impedance variations brought about by the tightness of the insulating jacket of a coaxial cable or vibrations in the braiding process of the outer shield [*Moffitt*, 1966] to catastrophic impedance

variations when, for example, a short between the inner conductor and shield occurs. In fact, assuming both conductors have the same resistance[3], the characteristic impedance (Z_O) for typical coaxial cable can be obtained using

$$Z_O = \left(\frac{138}{\sqrt{\epsilon}}\right) log_{10}\left(\frac{D}{d}\right) \tag{3.2}$$

where D is the outer conductor's inner diameter and d is the inner conductor's outer diameter [*Metzger & Vabre*, 1969; *Strickland et al.*, 1970; *Kennedy*, 1970; *Wadell*, 1991]. Thus most variation in these parameters over a finite length will give rise to a change in characteristic impedance and a discontinuity of some magnitude.

A significant proportion of the data presented in this Chapter was obtained using TDR techniques and various TDR equipment systems. Throughout the concentrated maintenance period which extended over six months there was a continual upgrading of the TDR equipment used as methods and techniques were improved and as specific equipment became available for use. While there were many different combinations of equipment utilised, large portions of the data were obtained using two main TDR equipment configurations and it is this data which is presented here.

All TDR equipment systems can be sub-divided into the test equipment and Device Under Test (DUT) components. The test equipment primarily consisted of a pulse generator, a Cathode Ray Oscilloscope (CRO) or Digital Storage Oscilloscope (DSO) and various patching cables. This system acts on or probes the DUT, for the most part being the Cable-Balun-Antenna sub-system but could equally be individual cables or components. The two main TDR equipment systems used are described in sections 3.2.1 and 3.2.2. The capabilities of each system affect the results acquired or place limits on the interpretation of the data. Factors influencing each system's capability are discussed, such as component and system risetime.

[3]This is realistic in the case of single strand conductors but less so for multi-strand conductors.

3.2.1 Equipment system I

The purpose of equipment system I was to provide TDR traces for immediate feedback on the status of the CBA sub-system under test. This information could then be used with data from other sources to form a picture of the most likely cause of the CBA faults or, if no faults were detected, to confirm it was performing to specification. In the event that a fault was detected, the TDR information could then be used to tailor the best approach for fault rectification. The emphasis here was to repair CBA faults in the least time thus enabling a majority of the array to be surveyed and made operational within the limited system down-time. Any TDR record could then be entered into the MF CBA Database (MF CBAD) for future use in tracking of individual CBA sub-system faults or for analysis collectively to form array maintenance overviews (refer to section 3.3.2). A secondary aim that utilised TDR traces obtained via equipment system I was to calculate cable electrical length in an effort to confirm its behaviour was within specification. This employed a TDR temporal measurement (labelled dX in TDR figures, Δt in text) and is more completely discussed in section 3.3.3.

The test equipment of system I comprises an Advanced Electronics PG58 pulse generator and a Tektronix TDS 210 Digital Storage Oscilloscope (DSO)[4] connected to an IBM compatible personal computer (PC) and printer. This in turn could be connected to any CBA sub-system via either antenna patchboard. A photograph of the experimental arrangement is shown in Figure 3.1 and the equivalent block diagram format in Figure 3.2.

It is important to establish the capability of the assembled TDR system and this can be explained in terms of the system's resolution limitations. In relation to TDR systems the term resolution is often used to describe the capabilities of different selected aspects of a system. For instance, resolution is often calculated as the display error of the accompanying DSO and excludes the characteristics of the pulse used and most importantly, the aspects of the device under test. The definitions outlined below attempt to incorporate all relevant aspects of a TDR system in an estimation of its

[4] 60 MHz bandwidth.

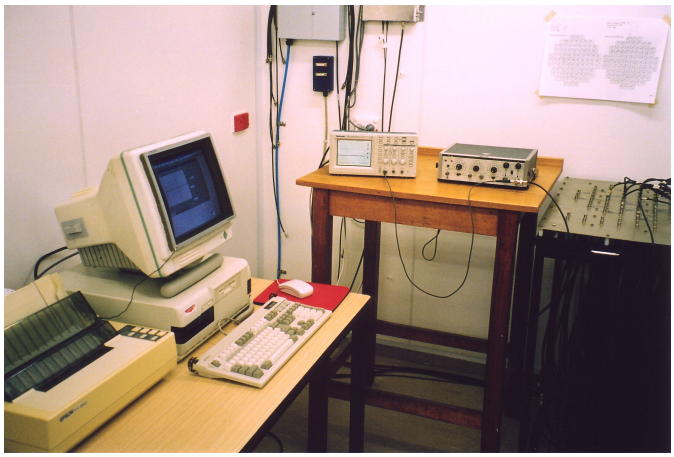

Figure 3.1: Photograph of TDR equipment system I. The system test equipment comprises printer (from left), IBM compatible PC, TDS 210 digital storage oscilloscope and AE PG58 pulse generator. This is connected to the device under test via the Cable-Balun-Antenna patchboard (far right).

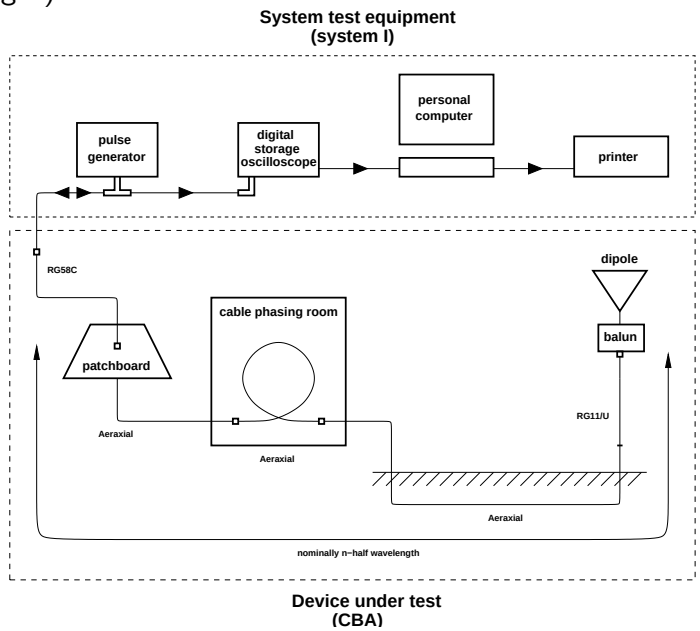

Figure 3.2: TDR equipment system I block diagram. This configuration was used for general documentation of 124 of the 178 cable-balun-antenna sub-systems. The test equipment comprises a Tektronix TDS 210 digital storage oscilloscope, AE PG58 pulse generator, IBM compatible PC and printer. The printer is connected to the PC via a parallel interface and the TDS 210 is connected to the PC via an RS232 interface. The test equipment probes the characteristics of the device under test. This device was commonly any cable-balun-antenna sub-system. It contains the feeder cable, antenna patchboard, Aeraxial coaxial cable (comprising cable phasing room and underground sections), Belden RG-11/U coaxial cable, balun and antenna. The cable phasing room houses excess cable required to achieve a nominal multiple half-wavelength section to the balun and antenna. Often a Belling-Lee connector has been inserted near the cable's transition to below ground level as an entry point for compressed air during water eradication procedures. Also, there may be other similar connectors used in patching various phasing sections. All connectors and cable sections must be included in estimates of equipment system resolution.

capability.

In general terms the resolution of a TDR system is basically the ability of a system to identify very small discontinuities (amplitude resolution) or identify two closely spaced discontinuities as having separate reflections (temporal/distance resolution) [*Strickland et al.*, 1970]. The varied treatment of temporal resolution of a TDR system in the literature is highlighted in the following discussion.

To better clarify the temporal resolution of a TDR system we will use the term *discrimination* to describe a TDR system's ability to differentiate two closely spaced discontinuities. This definition is more closely related to the optical term, *resolving power*, where the ability to resolve two objects angularly is required whereas here we resolve the two objects temporally.

Using this definition as a basis, the literature offers a variety of methods to calculate the discrimination based on the pulse width, system bandwidth or the system risetime used. *Strickland et al.* [1970] describes discrimination as the minimum time spacing of two equal point discontinuities which give rise to a 50% valley between the two displayed reflections, but offers no detailed account of the system parameters that influence this characteristic of a TDR system.

Grivet [1970] suggests that the resolving power is dependent on the pulse width used such that if two neighbouring irregularities that can just be distinguished from each other with a pulse of a set width (t_{pw}), then the resolving power (R) will be nearly equal to

$$R = \frac{c}{\sqrt{\epsilon}} \frac{t_{pw}}{2} \tag{3.3}$$

i.e. half the distance along the line during a time equal to the pulse length. Others reiterate this definition of discrimination (e.g. *BI Communications* [2001]) adding that half the pulse width (travelling in the transmission line) is the theoretical limit as the pulse is folded back in two at the point it bounces back off the discontinuity.

In a different approach *Davidson* [1978] suggests that the risetime can be determined from the bandwidth (BW) of the system, by applying $t_r = 0.35$ / BW, and if air spaced transmission line is assumed this can be related to a distance that will approximate a system's resolution capability.

A third approach focuses on the risetime of the applied pulse, rather that its pulse width, as the main source of discrimination limitation. This stems from the physical understanding that a slow pulse risetime will obscure returns from a discontinuity. *Andrews* [1989] suggests that the minimum temporal resolution is dependent on the system risetime (t_r) such that the minimum spatial resolution is given by

$$R = \frac{c}{\sqrt{\epsilon}} \frac{t_r}{2} \tag{3.4}$$

Moffitt [1966] also suggests that it is risetime that allows the identification of closely spaced discontinuities but initially follows a slightly different formulation. His analysis assumes the ideal case of the transmitted pulse travelling at the speed of light in the cable under test which is unrealistic in practical cable lengths but possibly achievable in air line. *Moffitt* [1966] and *Blonder & Evans* [1968] later include the relative dielectric constant of the cable under test for a more practical application to coaxial lines and their reasoning is discussed here. From Equation 3.1 it can be seen that the distance between adjacent discontinuities (D_{12}) in the same transmission line is given by:

$$D_{12} = D_2 - D_1 = \frac{c}{\sqrt{\epsilon}} \frac{(t_2 - t_1)}{2} \tag{3.5}$$

It becomes impossible to distinguish between the individual discontinuities when $t_2 - t_1$ is half of the system risetime (t_r). Thus the system resolution (R), in metres, is given [*Moffitt*, 1966; *Blonder & Evans*, 1968] by:

$$R = \frac{c}{\sqrt{\epsilon}} \frac{t_r}{4} \tag{3.6}$$

This is half the result of *Andrews* [1989].

It is apparent that an estimation of TDR system temporal resolution from either the pulse width or system risetime approaches has merit. In fact if pulse width is

defined as the time difference between the leading and trailing edge at the 50% level, this partially includes the effect of the rise and fall times of the pulse and highlights the close relationship between the two approaches. For the purposes of this study the pulse width and system risetime approaches were both used where applicable. Pulse width was varied in order to alleviate any masking of closely spaced discontinuities but was fixed at 210 ns for final TDR trace records in order to allow for a sufficient pulse return for consistent Δt measurements. Recommendations for pulse width (e.g. *Grivet* [1970]) suggest up to 100 ns for the cable lengths established at the Buckland Park site but this can depend on the number of discontinuities among other factors. The ability to resolve moderately spatially separated discontinuities is sought in this particular application of TDR to aid in efficient array maintenance by isolating and identifying the faulty component in a CBA sub-system. An estimate of system discrimination was calculated following the system risetime formulation.

If a system consists of various individual components, the system risetime is the risetime up to the point of measurement [*Blonder & Evans*, 1968]. Assuming that each system component degrades the risetime, then for N components the system risetime (t_r) is commonly (e.g. [*Hewlett-Packard*, 1965; *Blonder & Evans*, 1968; *Botos*, 1968; *Andrews*, 1989; *Agilent*, 2001*a*]) given as

$$t_r = \sqrt{\sum_{i=1}^{n} t_i^2} \tag{3.7}$$

The risetime t_i, for a component, is determined from the application of a rectangular pulse to the component.

For equipment system I (TDS 210 & PG58), if the risetime of each component can be estimated, then equation 3.7 can be rewritten as

$$\begin{aligned} t_{system\ I} = (&t^2_{scope} + t^2_{probe} + t^2_{BNC\ T} + t^2_{pulse\ gen} + t^2_{feeder} + t^2_{BNC\ patchbrd} \\ &+ t^2_{Belling-Lee} + (\triangle t_1^2 + \cdots + \triangle t_N^2) + t^2_{Aeraxial} + t^2_{RG-11/U} + t^2_{balun})^{1/2} \end{aligned} \tag{3.8}$$

where
t_{scope} = oscilloscope risetime
t_{probe} = oscilloscope's probe risetime
$t_{BNC\ T}$ = BNC T piece risetime
$t_{pulse\ gen}$ = generated pulse risetime
t_{feeder} = feeder cable risetime
$t_{BNC\ patchbrd}$ = patchboard BNC connector risetime
$t_{Belling-Lee}$ = cable phasing room connector risetime
$\triangle t_1$, ..., $\triangle t_N$ = difference in risetime before & after reflection 1, ... , N in Aeraxial cable
$t_{Aeraxial}$ = Aeraxial cable risetime
$t_{RG-11/U}$ = 10 m cable section before balun risetime
t_{balun} = balun risetime

This is the Time Domain Transmission (TDT) (one-way) risetime of the system if measured at the balun/antenna. The TDR (two-way) system risetime as measured at the DSO can be obtained noting that some components are encountered twice as the pulse traverses the system and thus some component values (t_i^2) can be doubled [*Hewlett-Packard*, 1965]. These are indicated by the inclusion of the various multipliers as noted in the Table 3.1.

Estimates of each component risetime that contribute to the total system risetime (t_r) needed to be made and these are tabulated in Table 3.1 and discussed in turn. The risetime of the DSO is given as <5.8 ns [*Tektronix*, 1993] (and by using the relation $t_{scope} = 0.35\ /\ f_{scope\ bandwidth}$)[5]. The risetime of the DSO probe (t_{probe}) depends on the selected attenuation of the probe. For a ×1 probe attenuation a risetime of ∼20 ns and for a ×10 attenuation ∼1.5 ns is possible. For the data collected a probe risetime of 20 ns is estimated [*Farnell*, 1998]. The risetime of the BNC T ($t_{BNC\ T}$) piece is estimated at ∼0.1 ns. The PG58 pulse generator was set to give a square pulse of frequency 4 kHz (period, $T = 250\ \mu$s), width ∼210 ns and delay ∼100 μs. Measured

[5]Risetime for oscilloscopes with bandwidth of < 1 GHz [*Matick*, 1969].

pulse risetime was 4.5 ns and pulse amplitude was approximately 5 Volts. The pulse delay, set here at 100 μs, is significantly longer than the longest cable length tested and thus limits any aliasing effects in the observed TDR trace. The feeder coaxial cable was primarily used to facilitate easy patching to the antenna patchboard and comprised two lengths of RG-58C coaxial cable totalling 3.63 m joined by a BNC connector. Its two-way risetime was estimated to be 0.6 ns. Again the risetime of the BNC antenna patchboard connector ($t_{BNC\ patchbrd}$) is estimated at 0.1 ns.

The cable phasing room houses the unburied excess lengths of cable required to make each section a nominal multiple half-wavelength. On any individual cable system there may be one or two Belling-Lee connectors used to allow insertion of these phasing sections. Also, to facilitate the eradication of water from the air-cored dielectric via compressed air, on many sections of underground cable a Belling-Lee connector was inserted in close proximity to the transition to the underground cable section. These extra connectors contribute only a fraction (0.1 ns each) to the total system risetime but are included for completeness.

As a pulse travels through a functioning transmission line, small to large discontinuities may increase the system risetime, depending on their individual characteristics. As stated by *Blonder & Evans* [1968], if the reflections across each discontinuity are small (i.e. less than 10%, and are frequency independent (i.e. pure, real impedances), the transmitted wave, in going through these discontinuities, is not degraded with respect to risetime. Thus, if the reflection across each discontinuity adheres to these constraints then the $\triangle t_1^2$,$\cdots$, $\triangle t_N^2$ terms can be neglected. However, if there are significant single or multiple faults along a cable with different characteristics, these *will* contribute to a degradation of pulse risetime and should be included in the overall estimate. A new or fully functioning cable can neglect these values.

An estimate of the isolated or cumulative effect of non-negligible discontinuities is difficult to obtain in the present system because the risetime of a discontinuity can only be best estimated by measurement immediately following the fault location with any other contributing component risetimes being removed. This would require a

substantial re-arrangement of equipment and technique to accomplish in the present survey. As a result, the effects on risetime of the primary cable discontinuities are neglected. This approach may affect the calculated system risetime by introducing a marginal underestimation, which should be noted when interpreting the results.

In order to calculate an estimate of total system risetime, an estimate for the Aeraxial coaxial cable risetime ($t_{Aeraxial}$) must be calculated for different cable lengths. This is a non-trivial task considering the age of the cables and lack of specification information[6]. This estimation is dealt with in a later section (refer to Appendix D) but the results indicate that this component's contribution to the overall risetime can be substantial. The two-way risetime of the RG-11/U type used for the 10 m section running up the antenna/balun pole is estimated at 1.0 ns. The risetime of the N-type connector at the base of the balun and the balun itself combined is 1.0 ns.

Component	**Risetime Estimate** [ns]	**Multiplier**
t_{scope}	5.8	1
t_{probe}	20.0	2
$t_{BNC\ T}$	0.1	2
$t_{pulse\ gen}$	4.5	1
t_{feeder}	0.3	2
$t_{BNC\ patchbrd}$	0.1	2
$t_{Belling-Lee}$	0.1	0,2,4
$\triangle t_1$,$\cdots$,$\triangle t_N$	negligible	-
$t_{Aeraxial}$	see caption	-
$t_{RG-11/U}$	0.5	2
t_{balun}	1.0	1

Table 3.1: Table of risetime estimates for components of TDR equipment system I. The Aeraxial risetime estimates ($t_{Aeraxial}$) vary for different length cables and are calculated from Equation D.1 discussed in Appendix D.

It should also be noted that Equation 3.6, which gives the resolution of the TDR system, is applicable for systems incorporating a single cable type with its accompanying constant velocity factor. In our case there is a mix of three distinct types of

[6]Note that some cable parameters can be calculated from known physical cable specifications.

coaxial cable used in TDR equipment system I with three distinct velocity factors, which significantly complicates the calculation. In order to apply Equation 3.6 in this case, it is assumed a single velocity factor value is representative of the system and is $VF = 0.79 = 1/\sqrt{\epsilon}$. This will have little effect on the resolution of the system in the context of the current application. This assumption is justified in the following way. The cable lengths incorporated into the system are estimated to consist of Aeraxial (49 to 528 m, $VF = 0.79$, see Table 3.7), RG-11/U (10.4 m, $VF = 0.78$) and RG-58C (3.63 m, $VF = 0.66$). If the Aeraxial and RG-11/U are viewed as equivalent because of their similar VF, then the length contribution of RG-58C (with its substantially different VF) to the total cable length ranges from 6% to 0.7%. Whilst having some effect on the resolution (R), the relatively small section of RG-58C that is present in the test equipment is deemed not to invalidate the use of Equation 3.6, with a nominal velocity factor, for an estimate of TDR system discrimination. Table 3.2 displays an estimate of the typical resolution encountered using TDR equipment system I for the range of cable lengths that compose the BP MF antenna array.

Nominal CBA Wavelength [λ]	**Discrimination Estimate** [m]
0.5	1·26
1.0	1·33
1.5	1·64
2.0	2·30
2.5	3·31
3.0	4·63
3.5	6·24
4.0	8·14
4.5	10·30

Table 3.2: Typical discrimination estimates (R) for TDR equipment system I when probing nominal wavelength cable-balun-antenna sub-systems. The estimate is calculated from Equation 3.6, with Aeraxial risetime estimated via Equation D.1 using nominal Aeraxial lengths given in Table 3.7. It was assumed that one Belling-Lee connector was present in the cable room phasing section for each estimate.

Related to the TDR system's ability to resolve two adjacent discontinuities is the

ability to observe *all* reflections from the Device Under Test (DUT). When a pulse is injected into the DUT the finite width of the transmitted pulse initially will obscure a distance equivalent to the pulse's width in that transmission line. This is commonly called the blind spot (e.g. *Electrodata* [2001]; *Bicotest* [1998]). The implication is that any faults or discontinuities that exist in this region will remain undetected. Two approaches to address this problem were used in both equipment configurations. To allow the pulse a distance to launch and to allow a flexibility in accessing the antenna patchboards, the aforementioned feeder cable was inserted before the cable of the CBA sub-system under test. This feeder cable length limited the extent of the blind spot in many cases but often the pulse width exceeded this distance (in order to obtain sufficient return for electrical length measurement in equipment system I particularly), so the pulse width was decreased in this situation to confirm no significant discontinuities existed in this obscured region of the cable.

While there are alternate definitions of discrimination in TDR systems, there is generally better agreement concerning a system's amplitude resolution or sensitivity. This refers to a TDR system's ability to display a reflection signal from a discontinuity that produces a very small reflection coefficient [*Strickland et al.*, 1970]. These authors go on to say that the amplitude resolution is primarily limited by system noise but in the case of a point discontinuity or one which is distributed over a short distance relative to the equivalent system risetime, the amplitude resolution is usually limited by both system noise and risetime.

Because the calculation of reflection coefficients inherent in inductive or capacitive discontinuities were not the focus of this study, the derivations for amplitude resolution (e.g. *Blonder & Evans* [1968]) are not included here. The amplitudes and pulse widths of the initial transmitted pulse in system I & II were sufficient to identify all discontinuities above system noise thought to have a significant bearing on cable performance. From the return pulse, measurements were taken to establish time intervals that allowed the calculation of cable electrical lengths which was a secondary aim of the system. In this respect the system amplitude resolution was adequate with any

measurement error brought about by varying amplitude levels thought to be negligible.

An example of typical output from TDR equipment system I is displayed in Figures 3.3 and 3.4. These two figures represent a before and after maintenance record of CBA sub-system 4E6[7] and are typical of those records in the MF CBA Database. Distinctive features of typical TDR traces are the large positive amplitudes on the extreme left and right of each figure, representing the initial (dashed cursor line) and balun return (solid cursor line) pulses respectively. Figure 3.3, taken on 16.3.98, shows evidence of water ingress into the air-cored dielectric of the Aeraxial cable indicated by the significant negative amplitude component of the trace preceding the pulse return from the balun. This water was removed (via compressed air techniques) and a further TDR trace taken on 24.3.98 is shown in Figure 3.4. This now represents a typical, fully functioning, CBA sub-system. It is interesting to note that the position of the return pulse is measured at 2.27 μs in the water affected cable and 2.02 μs after water eradication. This decrease in measured time after water removal is expected and is discussed in more depth in section 3.3.3.

Each TDR trace had a record length of 2500 points but a significant level of noise was encountered in the traces using equipment system I. This was partly due to the lengthy cable sections being probed and the initial amplitude of the pulse used, but is primarily due to the signal received on the connected dipole. In order to increase the SNR, each recorded TDR trace of a CBA sub-system was an average of 128 records and those TDR waveforms displayed here are windowed views of the averaged trace. It is also interesting to note that for a perfectly matched system all the initial pulse power at 1.98 MHz should be absorbed into the antenna balun, resulting in no return pulse visible at the 2.02 μs mark. As the CBA sub-system here is being probed with a 4 kHz signal, significant balun return is observed due to the mismatched impedance at this

[7]CBA sub-systems are labelled according to the direction in which radiation from the connected dipole attains a maximum, i.e. 4**E**6 indicates 4th array row, **east** patchboard, 6th array column with dipole physically oriented approximately north-south. Thus a maximum in dipole radiation occurs in approximately the **east**(-west) plane.

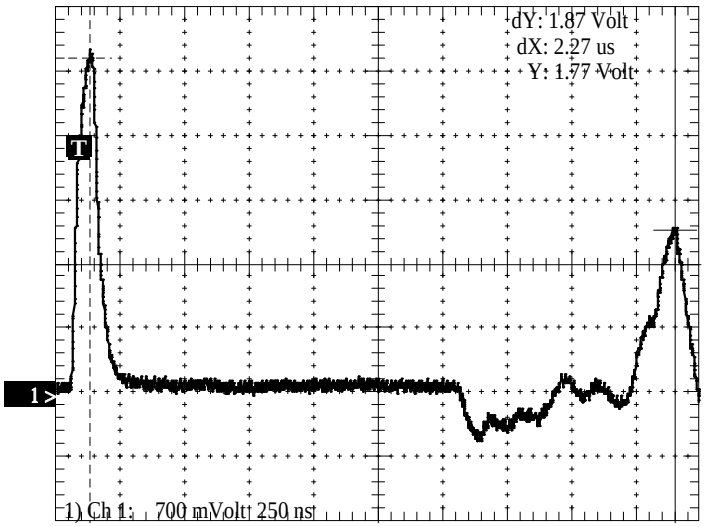

Figure 3.3: TDR trace of cable-balun-antenna sub-system 4E6 using equipment system I showing the presence of water ingress. The figure shows voltage (700 mV/div) against time (250 ns/div) with the T mark indicating the DSO trigger point. The time and voltage differences in cursor positions, labelled dX and dY, are shown in the upper right of the figure and are 2.27 μs and 1.87 V respectively. The negative amplitude structure of the waveform immediately preceding the balun return pulse is typical of a water affected underground cable section. Note that dX is later used as Δt in cable electrical length calculations.

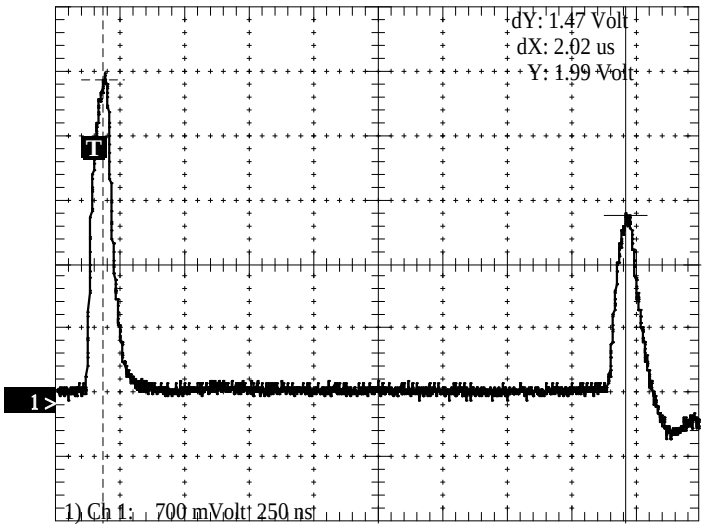

Figure 3.4: TDR trace of cable-balun-antenna sub-system 4E6 after water eradication via the use of compressed air techniques. The discontinuity free portion of the trace between the initial and return pulse indicates a fully functioning CBA sub-system. Note the decrease in dX value after water eradication from the coaxial cable.

frequency. Note that balun circuit tuning variation and varying antenna impedance will also lead to less than perfect power absorption at the balun, even at the matched frequency of 1.98 MHz. The fact that a significant return from the balun occurs at this probing frequency aids time interval measurement. Figure 3.8 highlights the alternate case where a matched load (at 4 kHz) absorbs all the initial pulse power. Such a situation makes time interval measurement much more difficult.

The Figures 3.5 to 3.12 on page 113 displays a sample of typical TDR traces taken during the Phase I maintenance period, representing often encountered faults or evidence of their solution. Each figure shows the initial pulse (dashed cursor line) and return pulse (solid cursor line) from the balun/antenna, with noted features. In general terms, the polarity of the trace provides information of the nature of the fault. A reflected pulse with a positive amplitude (increasing characteristic impedance) indicates an open circuit fault type, whereas a negative amplitude (decreasing characteristic impedance) indicates a short circuit fault type.

3.2.1.1 Improving equipment system I

Equipment system I provided useful documentation of the individual CBA sub-systems. The TDR records and analysis for the 124 antennas surveyed were used extensively in system fault finding and provided an invaluable record of the work completed that could be used for later collective fault analysis (see sections 3.3.2 to 3.3.4). However there were some deficiencies with this particular equipment configuration in terms of measurement technique and hardware.

The accepted optimum technique for TDR time (Δt) measurement, utilises the initial and return pulse leading edge at the point where the leading edge first emerges out of the system noise (e.g. *Grivet* [1970]; *Cole* [1977]) or at the 10% point (e.g. *Hewlett-Packard* [1965]). This minimizes the influence of distortions in the pulse itself, caused by pulse travel through the system components and past significant discontinuities, resulting in a more accurate temporal measurement. Affecting this Δt measurement obtained using equipment system I was the relatively low SNR of the traces recorded. The

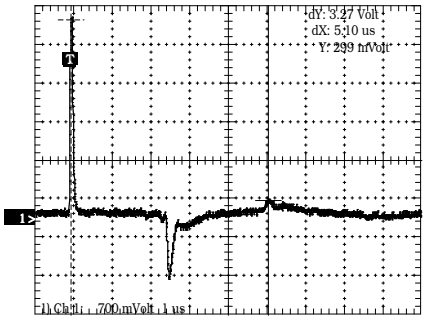

Figure 3.5: 10E8 shows a short circuit along the underground cable length.

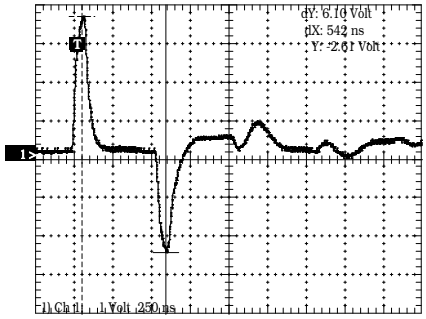

Figure 3.6: 6E6 shows a short circuit in the balun.

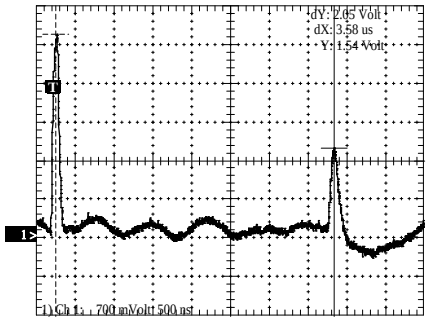

Figure 3.7: 8E3 shows a broken dipole feeder.

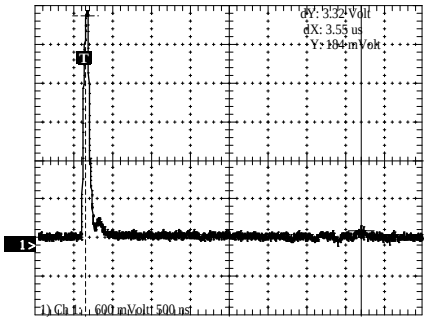

Figure 3.8: 8E3 with a 75 Ω load in place of the balun.

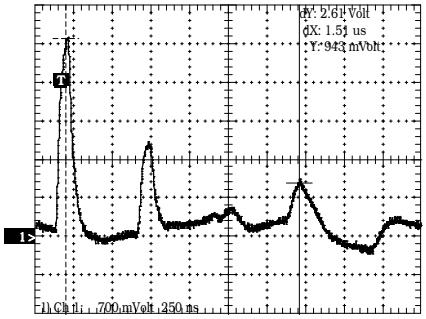

Figure 3.9: 5E5 shows an open circuit caused by a corroded joint in the field.

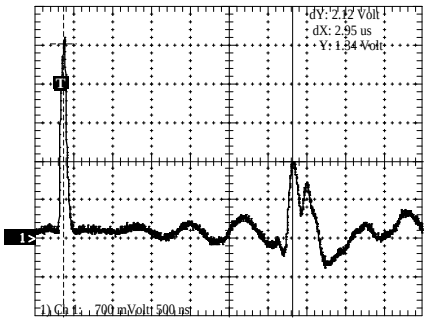

Figure 3.10: 3E7 shows an open circuit at the pole base.

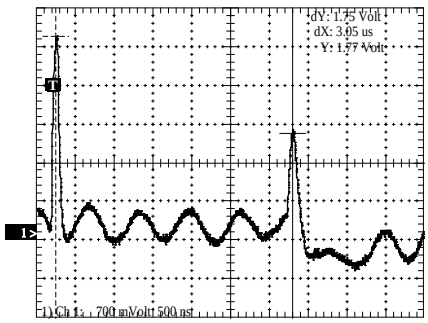

Figure 3.11: 9E5 shows a grounded dipole.

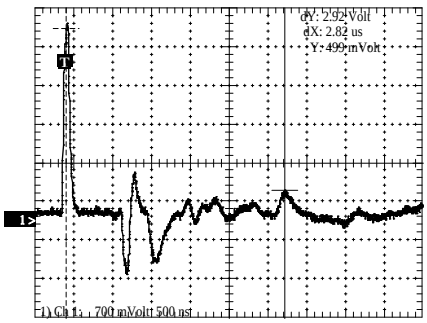

Figure 3.12: 5E4 shows a cable fault of unknown origin.

SNR was improved with the averaging of 128 waveforms for each recorded trace, but this still did not allow accurate identification of pulse leading edges in most cases. The use of the peak-to-peak measurement technique was substituted for temporal interval measurement and this is the method used in all Δt measurements using equipment system I. This method has the disadvantage that the actual measured peak location of a pulse can be significantly affected by reflections from closely spaced components within the system. In a lower resolution TDR system, the reflection observed is the sum of reflections that would be observed if each discontinuity was separated [*Hewlett-Packard*, 1964]. As an example, the pulse return from the base of the pole and balun/antenna often results in such a summation, with each individual reflection contributing a different magnitude that varies across CBA sub-systems. This results in a distortion of the peak component of the waveform and hence introduces errors in the measurement Δt using the peak-to-peak technique (see *Hewlett-Packard* [1965] for example). For the purposes of CBA documentation and general cable length calculation the magnitude of error introduced from the peak-to-peak measurement technique was deemed small as to be tolerable in the presence of other errors but should be addressed in future systems, where Δt translates to locations in the field and accuracy is needed.

Because the cable employed for the array is not of 50 Ω nominal impedance, interfacing the test equipment with any component not exhibiting 50 Ω characteristics presents impedance matching difficulties. Any impedance mismatch causes inefficient pulse power transfer at these boundaries resulting in signal distortions in the transmitted pulse and unwanted pulse reflections[8]. A consequence of this is that amplitude or voltage levels recorded are less representative of the system being tested, to the point that the voltages of the initial and return pulse can at best be used only as an approximation to current system performance and to the state of the CBA sub-system during normal radar operation. If the mismatches of the system are eradicated and the DSO probe calibrated the voltages will be representative of those inherent in the CBA sub-system.

[8]Normal radar operation, at 1.98 MHz, sees a more closely matched system.

The system discrimination places limits on the interpretation of the TDR trace. A commonly encountered problem, as described above, is where the often larger return pulse from the balun obscures any fault at the base of the pole or along the adjacent section of buried Aeraxial coaxial cable. This leads to time and resources allocated toward investigating the location of the fault rather that immediately rectifying the fault, whereas an increase in system discrimination would allowed better distinction of adjacent discontinuities.

The current system resolution can be improved via two approaches; system component re-arrangement and the reduction of the risetime of those remaining system components. First, the pulse generator can be situated before the DSO (e.g. *Elliot* [1976]; *Davidson* [1978]). This means the trace now recorded on the DSO is not affected by the return passage of the pulse past the pulse generator. Secondly, the resolution of the system can be improved by reducing the risetimes of the system components. For instance the DSO risetime may be improved by substitution of a wider bandwidth type, while a more capable (faster risetime) pulse generator could be used. Note that while DSO probe risetime can be manipulated by adjusting probe attenuation (increasing probe attenuation will decrease its risetime) this can affect the signal displayed by lowering the SNR, thus limiting the vertical scale accuracy and subsequently limiting accurate time interval measurements. In addition, the discrimination can also be improved by the further shortening of the pulse width provided enough energy is contained in the return pulse to allow effective parameter measurement to take place. It should be noted however, that system resolution in this application is ultimately dictated by the excessive cable length and the estimate for velocity factor of the CBA sub-system under test.

3.2.2 Equipment system II

The initial classification of faults in the CBA sub-system using equipment system I led to successful fault elimination in most cases. However, the isolation and location of faults in the underground section of the Aeraxial cable was beyond the capabilities

of equipment system I.

The specific task to be fulfilled by the revised equipment system (designated equipment system II) was to locate the position of underground cable faults. From the TDR trace of these underground cable faults, a distance over the terrain could be calculated and a cable locator could then be employed to isolate the fault's position in the field. Together with the techniques developed to accomplish this task, this system was viewed as a prototype system that could be used extensively in the future on any CBA sub-system in the array for fault rectification of similar type.

Those improvements mentioned in section 3.2.1.1 that directly contributed to the fulfilment of the main task of equipment system II were to be incorporated in this revised system. These improvements could be partly obtained by the replacement of the pulse generator and digital sampling oscilloscope with more capable (and now available) versions. Also, improvements could be made to the arrangement of the equipment.

In terms of components, both the pulse generator and the digital storage oscilloscope were replaced in the second equipment arrangement. Pulse generation was now provided by a Hewlett-Packard HP8112A pulse generator, which allowed greater flexibility in terms of pulse amplitude output and general operation (such as pulse width selection) but no significant change in pulse risetime performance. A Tektronix TDS 380 DSO[9] was used and has a specified risetime of 875 ps. TDR traces were stored electronically via the floppy diskette of the TDS 380 DSO for printing or manipulation at a later date. At the conclusion of the maintenance programme all TDR traces were archived to CDROM. General pulse parameters used were a square wave of frequency 4 kHz ($T = 250\ \mu$s) and a delay of 100 μs with a nominal peak-to-peak voltage of 10 Volts. This doubling of pulse amplitude compared to equipment system I contributed to a better SNR. Pulse width was selectable from 8 ns to 950 ms and was adjusted according to the length of cable probed (typically 8 to 3000 ns) and to allow closely spaced discontinuities to be revealed.

[9] 400 MHz bandwidth.

The layout of the equipment was revised in order to optimize the resolution of the system, which is vital for fault finding in the field. As outlined in the previous section the DSO was placed before the pulse generator in the system, primarily to reduce the system risetime. This eliminates the component risetime of the pulse generator and DSO probe cable being encountered by the return TDR pulse experienced in equipment system I. Also, the RG-11/U coaxial cable and the balun/antenna were excluded from the DUT by placing a short at the end of the Aeraxial cable. Thus the risetimes of these devices can be excluded from any calculation of system risetime. Each TDR trace was an average of 256 waveforms each containing 1000 points.

The calculated fault location along the cable using the increased resolution system was used in tandem with commercially available cable location equipment in order to isolate the fault in the field. Two cable fault locators were evaluated for this task, the PCI Pathfinder PF610 and the Dynatel 573AE. It was apparent that the PF610 was inadequate for cable location in long coaxial cables due to its lower generated signal strength as well as being logistically difficult to operate in the Buckland Park research facility environment. This led to the exclusive use of the more robust Dynatel 573AE system. This system uses a 300 kHz RF signal or low frequency audio tone coupled to the desired Aeraxial cable via an inductive loop or by direct connection at the patchboard or in the cable phasing room. A portable receiver tuned to the carrier frequency signal is then used to locate the specific cable in the group of buried cables at the location of interested indicated via TDR. This cable locator system is also capable of approximating cable depth via signal strength or simple triangulation methods, which can be an aid in cable excavation. The arrangement of components that constitute equipment system II are illustrated in the block diagram of Figure 3.13. The estimate of the TDT (one-way) system risetime could then be found from a revised version of Equation 3.7,

$$t_{system\ II} = (t^2_{pulsegen} + t^2_{25.5cm} + t^2_{BNC\ T} + t^2_{scope} + t^2_{feeder} + t^2_{BNC\ patchbrd} + t^2_{Belling-Lee} + (\triangle t_1^2 + \cdots + \triangle t_N^2) + t^2_{Aeraxial})^{1/2} \quad (3.9)$$

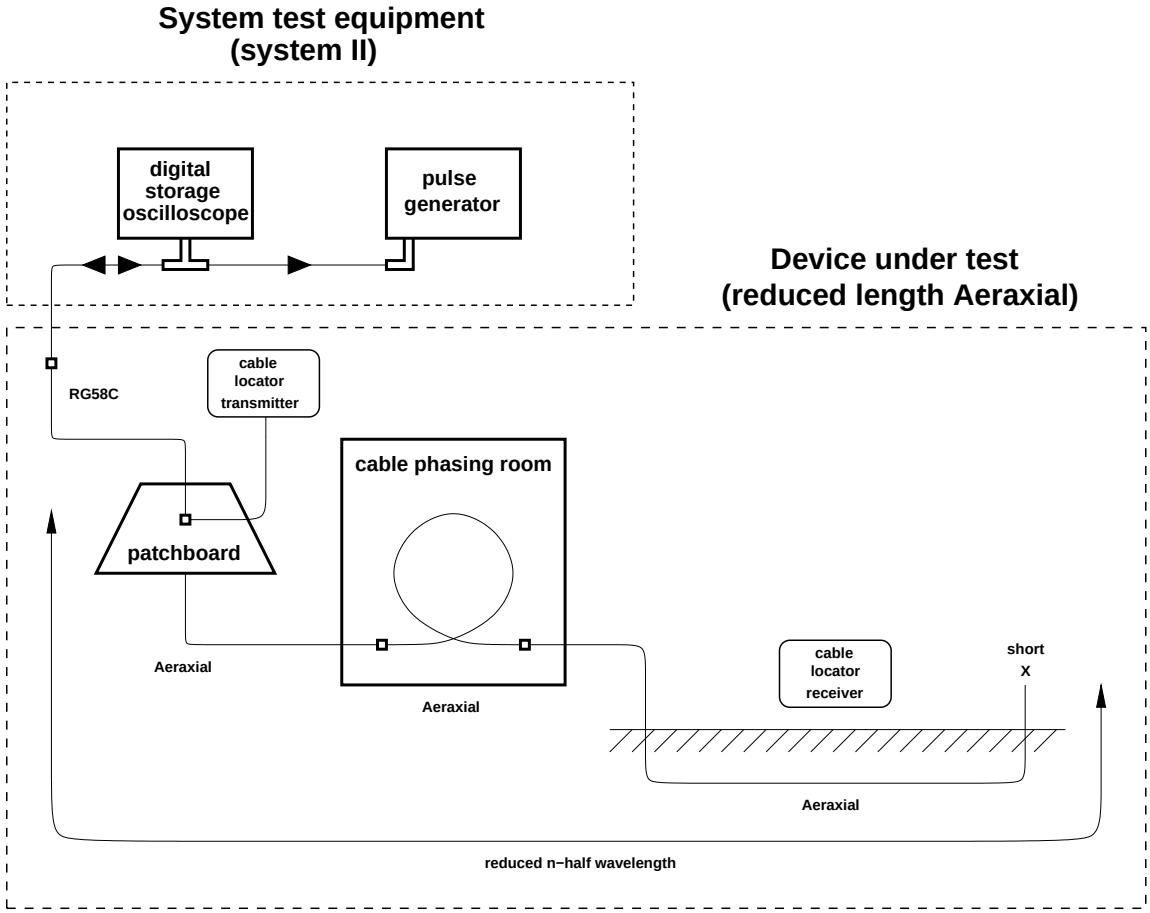

Figure 3.13: TDR equipment system II block diagram. This configuration was used for fault location along the underground section of coaxial cable. The test equipment comprises a Hewlett-Packard HP8112A pulse generator and a Tektronix TDS 380 digital storage oscilloscope. Alternatively connected to the patchboard was the transmitter of the Dynatel 573AE cable locator system. The manually operated cable locator receiver was used in the field in a region indicated via TDR. The device under test consisted of the feeder cable and the Aeraxial coaxial cable section (cable phasing room and underground sections). A short was placed at the end of the Aeraxial cable section.

where $t_{pulsegen}$ = generated pulse risetime

$t_{25.5cm}$ = patch cable risetime

$t_{BNC\ T}$ = BNC T piece risetime

t_{scope} = oscilloscope risetime

t_{feeder} = feeder cable risetime

$t_{BNC\ patchbrd}$ = patchboard BNC connector risetime

$t_{Belling-Lee}$ = cable phasing room connector risetime

$\triangle t_1, \cdots, \triangle t_N$ = difference in risetime before & after reflection 1, ... , N in Aeraxial cable

$t_{Aeraxial}$ = Aeraxial cable risetime

Estimates of the risetime of each component in this system are given below in Table 3.3 and the TDR (two-way) system risetime is again obtained with the inclusion of the multipliers in this Table. Note that the assumptions outlined in applying Equation 3.7 to equipment system I are suggested to apply equally for equipment system II. Table 3.4 displays typical system discrimination estimates for equipment system II. It can be seen that resolution estimates of equipment system II have increased from equipment system I levels as expected, although as cable length is increased the resolution gain

Component	**Risetime Estimate** [ns]	**Multiplier**
t_{scope}	0.875	1
$t_{25.5cm}$	0.05	1
$t_{BNC\ T}$	0.1	2
$t_{pulsegen}$	4.5	1
$t_{3.63m}$	0.3	2
$t_{BNC\ patchbrd}$	0.1	2
$t_{Belling-Lee}$	0.1	0,2,4
$\triangle t_1, \cdots, \triangle t_N$	negligible	-
$t_{Aeraxial}$	see caption	-

Table 3.3: Table of risetime estimates for components of TDR equipment system II. The Aeraxial risetime estimates ($t_{Aeraxial}$) vary for different length cables and are calculated from Equation D.1 discussed in Appendix D.

Nominal CBA Wavelength [λ]	**Discrimination Estimate** [m]
0.5	0·29
1.0	0·52
1.5	1·08
2.0	1·94
2.5	3·07
3.0	4·46
3.5	6·12
4.0	8·04
4.5	10·22

Table 3.4: Typical discrimination estimates (R) for TDR equipment system II when probing nominal wavelength cable-balun-antenna sub-systems. The estimate is calculated from Equation 3.6, with Aeraxial risetime estimated via Equation D.1 using nominal Aeraxial lengths given in Table 3.7. It was assumed that one Belling-Lee connector was present in the cable room phasing section for each estimate.

is reduced. Note that a small factor in this gain in resolution of equipment system II is the omission of the 10 m upright section of cable in the device under test. This increase in system resolution translates directly to a reduction in the labour expended unearthing any single cable. Examples of the TDR traces obtained from equipment system II, such as Cable-Balun-Antenna system 6E5, are displayed and discussed in section 3.3.4.

3.2.2.1 Improving equipment system II

While exhibiting a wholesale improvement in performance over the previous testing system, equipment system II required further optimization, both in technique and equipment components, to better fulfil its design purpose. Non-invasive TDR techniques, such as those used and described in section 3.3.4 with equipment system II, pose no risk to the integrity of the system being probed. Possible fault locations are calculated from TDR time intervals and the cable is visually inspected at these locations for obvious signs of damage. This technique relies chiefly on system resolution and on some physical indication of damage to the cable at the estimated fault location.

This approach has been found to be unsuccessful in precisely locating faults when applied to a limited number of buried cables in the field. A more aggressive approach is to introduce superficial faults to the cable around the estimated fault location in order to isolate a precise fault position. This technique is described in more detail in section 3.6. This particular technique reduces the need for a very high resolution measurement of the cable fault location that can then be related to a position over the terrain, as the introduced fault provides an immediate reference point. A disadvantage of this technique is that it runs the risk of permanently damaging fully-functional sections of cable around the known fault and can then allow a direct entry point for water ingress.

An alternative to the invasive approach outlined above is to further increase the system discrimination by lowering the transmitted pulse risetime. Pulse risetimes of picosecond order are achievable and are an order of magnitude better than those used in equipment system II. Of benefit also, in terms of system resolution, is to further isolate the particular cable sections of interest. Here, the system test equipment could be connected to the underground section of cable at the last Belling-Lee connection before its transition underground. As this arrangement reduces the length of Aeraxial cable probed via TDR, an increase in system resolution is encountered by elimination of the response of the cable phasing sections and less significantly from the omission of other connectors. This will also simplify cable measurement in the field by eliminating the need for an estimate of the physical length of cable in the cable phasing sections, which are inherently difficult to measure accurately (due to their coiled form). Impedance matching in this situation could be achieved by a network of resistors inserted between the DSO and the beginning of the underground cable section such as that described in section 3.6. This approach adheres to the TDR system design principles of using a minimum of circuit components and maintaining impedance characteristics between them [*Cole*, 1977]. A disadvantage of this technique is the non-ideal environment (both in terms of equipment and human factors) of the cable phasing room for extensive periods of maintenance work.

Because the TDR signal normally varies over time periods much greater than those used to capture the TDR trace a significant increase in the number of averaged waveforms may benefit parameter estimation without any fear of obscuring time dependent features. Increasing waveforms averaged by an order of magnitude (to 1024) over equipment system I levels will yield an improved an SNR of the TDR traces. With modern digital storage oscilloscopes this may be accomplished within hardware or later via software manipulation of the raw data files.

The employment of both TDR systems has called into question whether the commonly applied relation for system risetime (Equation 3.7) is the most appropriate description. *Hewlett-Packard* [1965] point out that this equation is best applied to short cables assuming a Gaussian response. Similarly, *Botos* [1968] indicates that the equation provides a valuable guide for general use but warns that the relation only applies strictly if the pulses are Gaussian in shape and provided there is no overshoot. More seriously he points out that coaxial cables exhibit behaviour divergent to these constraints. So while it can be assumed that connectors and other minor system components may follow a Gaussian frequency distribution, lengthy (cascaded) coaxial transmission lines should not be included in this group.

This situation is compounded as the response of the Aeraxial cable sections of the CBA sub-system rapidly become the most significant component affecting overall system risetime as cable length increases. Further complications arise in terms of the diversity of coaxial cable type available and hence their varying characteristics. The dramatic effect that the cable can have on total TDR response has been observed previously [*Editorial*, 1974]. So the incorporation of this parameter into the estimation of system resolution is vital if an accurate estimation of system resolution is to be obtained. How cable response could best be included in an estimation of system risetime is a complex question. Rather than approach this from a theoretical perspective the following paragraph describes an experimental approach to estimate the system resolution.

A more complete approach to determining the risetime of a test step within a

complex system of components, including those exhibiting non-Gaussian distributed characteristics, could be utilised. To best obtain an estimate for the risetime of a test step *Botos* [1968] suggests using a TDR system to observe the reflection from a short at the point of interest. *Andrews* [1994] suggests a similar arrangement but stresses that to establish the behaviour of a pulse within a system any measurement of interrogating pulse behaviour should occur at the plane where all future measurements will take place. While this approach will better establish the risetime of a complex TDR system any practical implementation of this technique into future maintenance programmes will be influenced by a number of concerns. Establishing consistent interrogating pulse behaviour in long coaxial cables can be difficult due to its dependency on pulse width (refer to Appendix D) and the variability in performance of individual cables exhibiting faults along their length. Also, labour and time expended establishing system risetime estimates using this procedure could be better directed toward actual fault rectification. Finally, efforts to avoid further damage to the cable integrity would preclude the introduction of a short at the point of interest for the sole reason of determining the discrimination achievable on that particular cable. These concerns dictated that no time in the current maintenance programmes was devoted to system risetime estimates using this technique but future, limited, cable investigations may incorporate it.

Further flexibility in data storage and manipulation may be attained by the re-introduction of a PC and printer in a future system. TDR trace manipulation software is useful in the interpretation of faults along CBA sub-systems, while immediate hardcopy output of TDR traces is useful in establishing a history of individual CBA sub-systems. A third generation TDR system is more completely described in the section 3.6. Data collected using the two TDR systems described in this and the preceding sections is discussed next.

3.3 Data

The current period of extended array maintenance allowed attention to be focused on five areas of interest. This section details the data collected in terms of these interests.

Two important areas for attention initially were the estimation of Aeraxial coaxial cable velocity factor (VF) and risetime ($t_{Aeraxial}$). The estimation of Aeraxial velocity factor was to have a direct application in the calculation of cable lengths, and the rise-time played a significant part in determining the TDR system resolution. These points, coupled with the absence of comprehensive data on the Aeraxial type of cable which constituted the major portion of the MF antenna array, led to a brief investigation of applicable estimates for them.

A third area of interest is the causal distribution of faults throughout the array. All individual CBA sub-system records were examined over the antenna maintenance period and the faults encountered were classified into Cable, Balun or Antenna area problems. This is instructive in gaining an appreciation of whether past upgrades to the CBA sub-system were effective and in locating where the future array maintenance problems may lie. This information is then collated to form a current picture of the operational status of 124 of the 178 antennas of the array.

An investigation into the behaviour of the Aeraxial electrical cable length with its air-cored dielectric alternatively affected and then unaffected by water ingress was undertaken in order to validate past and present maintenance practices. It was expected that a section of Aeraxial cable affected by water ingress would result in an increase in a calculation of cable electrical length when compared to the same section in an unaffected state. Similarly, calculated atmospheric phase error values were expected to indicate cable sections affected by water ingress. Results of these investigations have direct application to future array maintenance practices. Also a more detailed investigation of a specific CBA sub-system (i.e. 6E5) was undertaken with equipment system II in order to locate faults in the field. Work in each of these areas is discussed in turn in the following sections.

3.3.1 Coaxial cable velocity factor

The speed of propagation of information in a transmission line with respect to the speed of light is termed the velocity factor (VF) and is often expressed as a percentage. In the TDR techniques used here it is an important characteristic of coaxial cable because it directly affects any length or fault location calculated.

The coaxial cable used for the underground sections of the array was Aeraxial type A Mark II polythene[10] sheathed coaxial [*Rossiter*, 1970], with a nominal impedance of 75 Ω. *Vandepeer* [1993] noted the VF of this cable as 0.8 and impedance 70 Ω, but was often found to vary above this nominal impedance value. *Rutherford* [1996] has used commercial TDR devices to estimate the Aeraxial cable velocity factor and has determined values significantly lower than 0.8. Manufacturer specifications could not be found on this type of cable to confirm any of these values. It is also noted that for any given cable specifications, an individual cable's characteristics can vary from one manufacturer to another and over consecutive productions runs. It has been suggested that variations of up to 10% can be encountered [*Straw*, 1994; *King*, 1989]. Also, the cable is over 30 years old and some deterioration in performance has most likely occurred.

It is unlikely that a VF of 0.8 accurately represents each cable's value. Also it is assumed that a VF of any cable will be at or below the nominal VF factor due to cable deterioration. A slight decrease in VF, such as 2.5%, can have a significant effect on calculated coaxial cable physical length at 1.98 MHz. For instance Table 3.5 illustrates the magnitude of the length differences (Δ) of wavelength multiples of coaxial cable when two similar but distinct VF values are used. The increasing magnitude of the differences with small VF variation has a direct bearing on the ability to easily find the location of a fault in the field, as inaccurate fault positions due to small variations in VF dramatically increase the time required to physically locate the fault position. This translates to a greater time and cost spent in locating cable faults. It is because of this that a brief study of the velocity factor of the Aeraxial cable was undertaken

[10]Polythene is a commercially used name for polyethylene [*Grivet*, 1970; *Hughes*, 1997].

to determine which of these values was more representative. Five examples of the

Wavelength [λ]	**VF**	**Physical Length** [m]	Δ [m]
0·5	0·78	59·05	
	0·80	60·57	1·52
1·0	0·78	118·10	
	0·80	121·13	3·03
1·5	0·78	177·16	
	0·80	181·70	4·54
2·0	0·78	236·21	
	0·80	242·26	6·05
2·5	0·78	295·26	
	0·80	302·83	7·57
3·0	0·78	354·31	
	0·80	363·40	9·09
3·5	0·78	413·37	
	0·80	423·96	10·60
4·0	0·78	472·42	
	0·80	484·53	12·11
4·5	0·78	531·47	
	0·80	545·09	13·62

Table 3.5: Magnitude of length difference in Aeraxial coaxial cable due to two similar, but distinct velocity factors. Column one is a nominal wavelength multiple representative of those found within the MF antenna array cable system. The physical length of an electrical wavelength (λ) of cable is given as $\lambda = (c \times VF)/f$ and the case for various nominal wavelengths can be found by using $(n+\frac{1}{2})\lambda$. The difference between the two physical lengths (Δ, in metres), using the two distinct VF, is displayed. Note that the lengths displayed represent the case for a coaxial section of one cable type only. The current complete cable sections of the BP MF antenna array consist of two distinct cable types.

Aeraxial cable, with lengths ranging from 9.284 to 58.310 m, were tested. These example lengths were surplus off cuts of the original cable used. The velocity factor can be determined via Equation 3.10;

$$VF = \frac{2\,CL}{c\,t} \tag{3.10}$$

where CL = cable length, in m

c = speed of light, in m/s

t = pulse two way time, secs

If the quantities come from a normal distribution then the error in VF (ΔVF) can be estimated using Equation 3.11.

$$\triangle VF = VF\sqrt{\left(\frac{\triangle CL}{CL}\right)^2 + \left(\frac{\triangle t}{t}\right)^2} \tag{3.11}$$

The Figure 3.14 displays the results of this investigation.

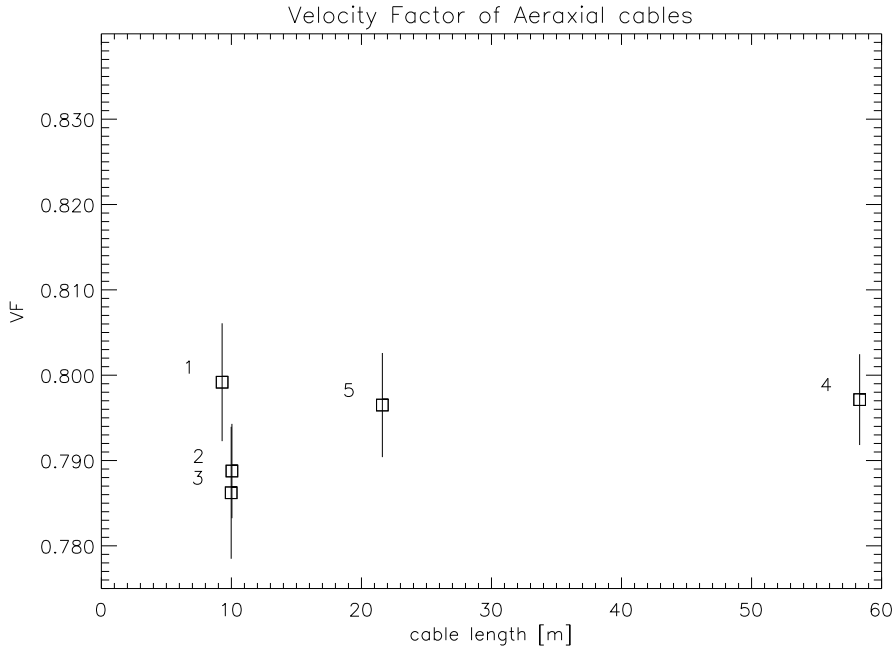

Figure 3.14: Determination of Aeraxial coaxial cable velocity factor.

If this small sample of cables were cut from a single cable length or were from a similarly manufactured batch we expect the calculated VF values to be distributed normally about a fixed VF between 0.78 and 0.8. Cables (1), (4) and (5) could be interpreted as belonging to the same batch (i.e. same VF value) within errors, but cable (2) and (3) may have come from a different batch. Note also that cables (1), (2), (3) are of similar length, yet (1) has a distinctly different VF factor. It is likely that cables with differing velocity factors are present in this small sample and this situation is likely to be representative of the cables that compose the complete array.

In fact anecdotal evidence [*Wild*, 1998, private communication] suggests that each cable length had a specific velocity factor that was noted by the manufacturer on each cable reel delivered to the Buckland Park site during array construction. This would

appear to be consistent with the results presented above. Unfortunately records of these values are unavailable at this time and a VF representative of the Aeraxial cable is required for later cable length calculations. A VF of 0.790 ± 0.016 was assumed for further calculation of the Aeraxial cable length.

It should be noted that a more complete approach to the problem of VF determination would be to measure each cable run and deduce the VF factor individually. However, ascertaining the actual physical length of each cable would be a time consuming task on an array of this size and each value would undoubtedly have a non-negligible error associated with it due to the need for various estimates for the physical length of the buried and coiled cable sections. It seems that an estimate for a commonly representative VF and its associated error is the best course at present, but this approach should be noted in the interpretation of later results. Particularly, the later calculated theoretical and experimental electrical lengths may not be best interpreted as absolute cable length values but better interpreted as relative values. While the velocity factor known to a high precision reduces the uncertainty in the location of faults in the field it is not as critical in electrical cable length calculation for purposes of water ingress comparisons. In this situation emphasis is on a relative difference between cable lengths and variations in a representative VF will not adversely affect the resulting difference between water affected and non-water affected cable lengths. The estimation of cable risetime is also of importance to the current investigation and this is more fully discussed in Appendix D.

3.3.2 Cable, balun and antenna sub-system survey

A maintenance programme for the antennas in most need of attention was devised and implemented. The primary aims of this programme were firstly, to correct all CBA faults in an effort to approach 100% array operational status and secondly to obtain data on the nature of the faults encountered that could be analysed with a view to improving general array maintenance procedures. A summary of the data collected throughout this first maintenance period is presented in this section.

With initial data from the methods outlined in section 3.1, details of the maintenance programme could be constructed. While the timing of the lightning strike that disabled the transmitting and receiving equipment was unforeseen, it occurred just prior to one of the two ideal periods of the year that array maintenance can best be performed, autumn and late spring. Aside from the ever-present restriction on maintenance periods that a continuously operated remote-sensing device exhibits, another primary restriction on any maintenance period is environmental. Winter and early spring pose array maintenance difficulties due to the poor water drainage from the site, which is partially caused by the site's low elevation. This limits vehicular and supporting structure activity. In contrast to this, the daytime temperatures during summer regularly approach and exceed 40°C which similarly limits much activity at the site. Thus maximum use of the autumn period was instituted, with maintenance progressing through winter as opportunity provided.

The maintenance of the antennas was divided up into two phases. Maintenance Phase I would address the immediate need for functioning antennas and Phase II would investigate possible techniques for use in correcting significant, long standing cable problems of selected individual antennas or those more serious problems found by Maintenance Phase I. This structure of maintenance programme was thought to be the most effective approach for a number of reasons. The antenna array, up to this point, was in near constant operation and required the use of in excess of 60 transmit/receive antennas, thus establishing a minimum need for readily available antennas. Further, maintaining only a minimum number of antennas severely restricts transmission and reception flexibility. As atmospheric observational demands fluctuate, the restriction imposed by maintaining only a minimum number of operational antennas precludes easy array configuration while also limiting its potential application. Secondly, records of faults existing or developing on specific cable runs had been accruing over some time. Solutions to these types of problems were not immediately evident and they required a more concentrated focus of attention that was outside the scope of the first Maintenance Phase.

The data collected within each antenna Maintenance Phase is discussed separately. The following paragraphs and section 3.3.3 outline that data collected during Maintenance Phase I and section 3.3.4 discusses the data collected during Maintenance Phase II.

Specifically, the objective of Maintenance Phase I was for CBA sub-system operation ability via each system having a patchboard measured complex impedance of $|Z|=75\pm15\ \Omega$ and $\angle Z=0\pm15^{\circ}$[11] and a TDR measurement to confirm it is free of serious discontinuities. This TDR record is then entered into the CBA database. Also, a verification of TDR measured electrical cable length as compared to theoretical cable length was used to confirm the veracity of any fault corrections. This is more comprehensively discussed in the next section.

Maintenance Phase I utilised equipment system I described previously in section 3.2.1 and was sub-divided into three groups of antennas in descending order of importance. Group I: (antennas connected to) Tx/Rx channels 1 to 10, Group II: assorted central antennas, Group III: (antennas connected to) Tx/Rx channels 11 to 20 as well as other non-central antennas marked as faulty.

CBA sub-systems connected to Tx/Rx channels 1 to 10 held priority in the maintenance schedule because of their role in maintaining core radar observations. The assorted central antennas were given a higher priority than the channel 11 to 20 and outer antennas because of their shorter cable lengths to each dipole. This translates to a greater transmitted power from these central dipoles which reduces system losses on transmission and reception. Thus maintaining all central antennas is a key tool for use in any array optimization programme. Further advantages of maintaining the central section of CBA sub-systems is that any transmission arrangement uses a significant proportion of these dipoles in order to produce a near symmetrical, narrow beam-width, polar diagram.

[11] Acceptance ranges for the complex impedance (Z) of CBA sub-systems measured at the patchboard of the MF array at the Buckland Park field site have emerged out of continuous monitoring and specific studies (e.g. *Vandepeer* [1993]).

As each balun in the array was the connection point for two dipoles (oriented NS and EW) and thus two underground cable runs, it was deemed an efficient use of time to examine both systems at once if one CBA sub-system was marked as faulty. The selection of this approach was primarily due to the considerable time spent to relocate test equipment in the field, but also to take advantage of the fact that each balun accessed two identical length cables which could be used for inter-comparison in fault finding.

Also, any fault that arose during the scheduled maintenance period on previously attended to CBA sub-systems, either new faults or re-occurring ones, were attended to and included in the survey. The periods of the two Maintenance Phases and their sub-groups are outlined in Table 3.6. The table indicates that most antennas were surveyed during autumn, then as weather permitted.

Whereas Maintenance Phase I was directed at the implementation of known solutions for each encountered fault, Maintenance Phase II sought to investigate all CBA sub-systems with significant cable faults for the nature of their faults, tailor a solution and initiate repair.

Maintenance Phase	**Group**	**Period**	**Total Cable-Balun-Antenna Surveyed**
I	I	4.3.98 → 4.6.98	68
	II	29.5.98 → 23.6.98	26
	III	23.6.98 → 13.8.98	30
II	I	18.8.98 → 31.8.98	6

Table 3.6: Cable-Balun-Antenna maintenance programme periods and totals of CBA sub-systems surveyed.

As each CBA sub-system was repaired the nature of the fault was recorded in the CBA database and its operational status assessed. Faults not immediately repairable, such as cable shorts between the inner conductor and shield or un-classifiable faults,

were short-listed for Phase II of the maintenance programme. The cumulative results of Phase I maintenance are presented in the following two distribution charts.

Figure 3.15 illustrates a summary of the Cable-Balun-Antenna faults encountered during Phase I maintenance. Some 124 CBA sub-systems were examined out of a total of 178. However this sample included four CBA sub-systems that were re-surveyed during the maintenance period due to their development of further faults. Thus, the survey covered approximately 67% of the MF antenna array. A total of 144 faults in the CBA sub-systems were found, with the faults classified primarily according to their respective Cable, Balun or Antenna groups. The chart is colour coded to differentiate the Cable, Balun or Antenna groupings of the fault and to allow later comparison where possible with the previous work of Vandepeer. Water intruding into

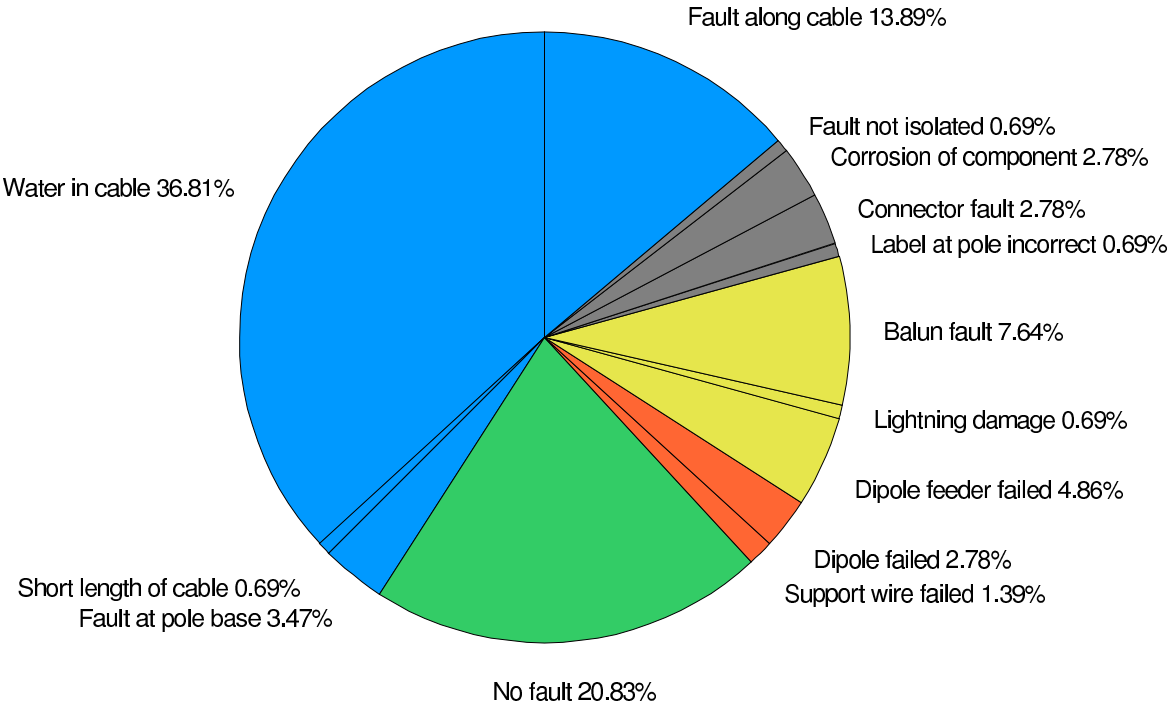

Figure 3.15: The Cable-Balun-Antenna (CBA) faults encountered during the Phase I maintenance cycle. A total of 124 CBA systems were examined and 144 faults logged. Faults pertaining to the major individual parts of the CBA sub-system are colour-coded: Cable (blue), Balun (yellow) and Antenna (orange). Faults not grouped in any of the three main classifications are represented by Miscellaneous (grey), with No Fault (green). The relative percentage of each individual component is also displayed. It can be seen most faults are detected in the cable system with water intrusion the most common problem. Total fault percentages for the primary sub-systems are Cable (54.86%), Balun (13.19%) and Antenna (4.17%).

the air-cored dielectric of the cable is the most common fault.

The next two main individual sources of faults were faults or discontinuities along the cable (13.89%) and faults in the balun unit (7.64%). The cable discontinuities were earmarked for Maintenance Phase II and as such are discussed more thoroughly in section 3.3.4.

Balun unit faults are confined mostly to failed silvered mica tuning capacitors or capacitors values that no longer tune out the reactive component of the dipole. Secondarily, the feeders that interface directly to the dipole also exhibit a significant failure rate. The cause of this is due mostly to the development of a dry joint in this connection, thought to be from its exposure to the harsh coastal environment.

The operational status of each CBA sub-system was evaluated at the conclusion of all maintenance procedures using primarily the data collected during the current maintenance cycle with some reference to the available historical records of each CBA system. Cable sections displaying small discontinuities, barring any other significant effects (such as poor antenna impedance etc.), were deemed to be useable but noted for further attention at some later stage. Such cable faults were thought to have a negligible adverse effect on any data collected. A distribution of the operational status of the CBA sub-systems encountered at the conclusion of Maintenance Phase I is displayed in Figure 3.16. This indicates the level of operation ability that can be achieved using the established methods of fault rectification and provides a current list of antennas that could be used for transmission or reception in any required arrangement. Similarly, it also highlights the level of those outstanding problems which may require new techniques to address. The CBA sub-systems classified *Not operational* consisted mostly of faults along the underground cable section. These faults can be difficult to rectify at the current time (see sections 3.3.4 or 3.6). Of the 32% *Operational, but fault(s)*, most have discontinuities along their cable lengths. The majority of these faults are considered minor at the present time, but it is possible that some of these faults may become more serious leading to the unavailability of a CBA system.

The mechanism by which the fault develops is thought to follow numerous paths.

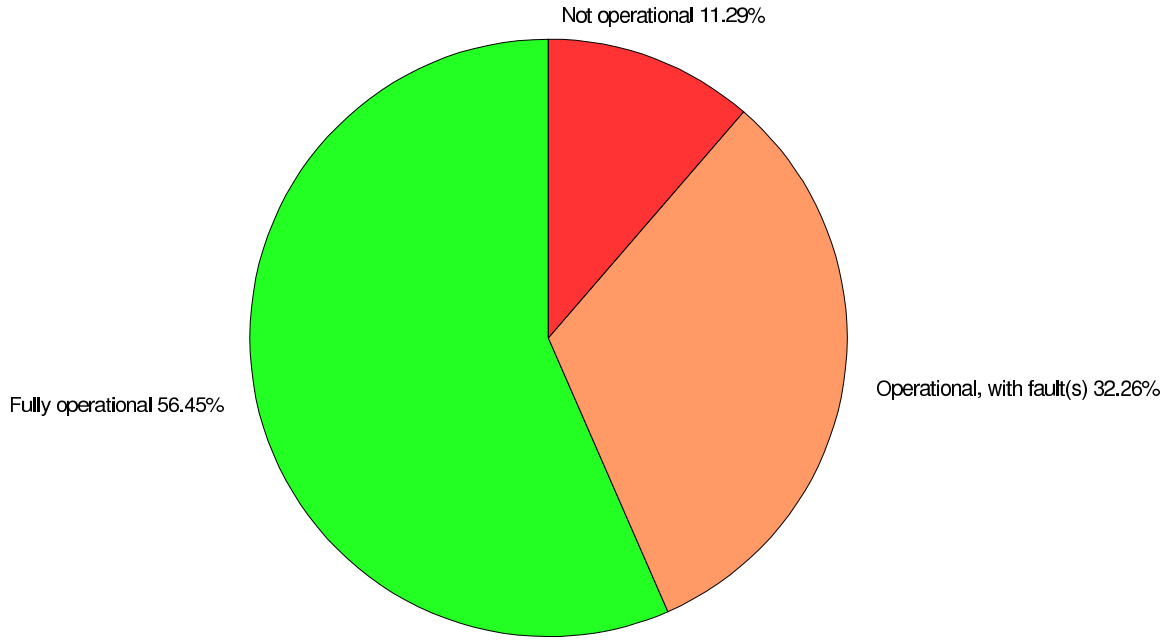

Figure 3.16: Shows the status of the surveyed Cable-Balun-Antenna sub-systems at the conclusion of the Phase I maintenance cycle. A total of 124 antennas were examined. Each system is classified as one of Operational (green), Operational with fault(s) (orange) or Not operational (red). Percentages of the components are also displayed. A majority of the *Operational, with fault(s)* CBA sub-systems have minor cable discontinuities.

The initial discontinuity may be due to vermin activity or deterioration of the cable sheath, then dielectric etc., which then may be exacerbated by the corrosive action of the salt air and water environment. It is probably prudent to investigate these faults before they become more difficult to repair. If the cable is left to deteriorate a new cable section will need to be inserted as a replacement. This will introduce amplitude and phase behaviour within the cable divergent from that of the majority of the array that haven't had the integrity of their length breached.

As mentioned above, many *Operational but fault(s)* have cable discontinuities as their sole fault. This relatively high percentage is not reflected in the lower percentage of *Fault along cable* of Figure 3.15 because a significant percentage of cable discontinuities are only revealed when water is eradicated.

3.3.3 Coaxial cable electrical length using equipment system I

The calculation of the electrical length of coaxial cable from its electronic response can be a useful tool in monitoring the behaviour of the extensive network of cables that compose the feeders to each antenna in the array. Some preliminary investigations of electrical cable length had been completed using a frequency of impedance method, incorporating measurement of frequencies at which impedance minima and maxima occur along a shorted cable [*Briggs*, 1977]. At the time this method required laborious frequency sweeps of selected cable sections. Alternatively, *Holdsworth & Rutherford* in 1996 applied the Pulse TDR method in their preliminary studies of cable length and attenuation. However no previous use of TDR techniques on the MF antenna array post array installation had incorporated an extensive, systematic calculation of cable lengths and subsequent check for water. It was thought the application of the Pulse TDR method to obtain cable electrical length of individual CBA sub-systems included in the Phase I maintenance survey would provide a comprehensive data set from which conclusions could be drawn.

It was thought necessary to detail a use of electrical cable length values and validate the accompanying technique as an effective indicator of cable faults that can be applied alone or together with other fault description tools. Specifically, we wanted to show that a calculation of theoretical cable length compares well with a TDR derived cable length from a fault free cable. Such a comparison can then be confidently used as evidence for a cable section performing up to specification. Further, if water has ingressed into a cable, an increase in the TDR derived electrical length will be found (expecting that the larger volumes of water exhibit an even larger recorded length). If this water is then excluded from the cable and no other faults are present, the TDR cable length again approaches its theoretically calculated length. Evidence for these propositions are shown in the following paragraphs. Another often used indicator of CBA sub-system ailments was atmospherically derived system phase error values. The correlation between these values and water affected cable lengths is studied with

a view to validating the current method employed. The results of this investigation and advice on future implementation are also detailed in the following paragraphs.

An estimate of the cable length from theoretical considerations was first sought for later comparisons. The original nominal theoretical lengths and layout of the complete cable system to each balun box is given in *Rossiter* [1970, Figure 3.4] and *Vandepeer* [1993, Figure 2.3(a)]. These figures show wavelength multiples (0.5 to 4.5) of electrical cable length in terms of the 1.98 MHz transmit frequency. Until the array upgrade period of 1992/94 each length consisted totally of the Aeraxial type cable. However the implementation of improvements suggested by *Vandepeer* [1993] required the replacement of the ten metre section of coaxial cable that ascended the dipole pole support in order to alleviate the water entry point and subsequent channelling into the underground cable section. This means that the there is now a reduced wavelength section of Aeraxial cable together with an approximate 10 m section of Belden 8213 RG-11/U added before the balun box.

Typically, a 10.4 m section of RG-11/U was used. So the remaining wavelength and physical length of Aeraxial cable can be calculated. This is shown in Table 3.7. Due to this mixing of coaxial cable types since the upgrade period it is now more

Nominal Wavelength [λ]	**Reduced Aeraxial Length (T)** [λ]	**Reduced Aeraxial Length (T)** [m]
0.5	0.413	49.4
1.0	0.913	109.2
1.5	1.413	169.0
2.0	1.913	228.8
2.5	2.413	288.6
3.0	2.913	348.4
3.5	3.413	408.2
4.0	3.913	468.1
4.5	4.413	527.9

Table 3.7: Remaining theoretical Aeraxial cable lengths.

accurate to refer to the complete cable electrical wavelengths as nominal values.

As mentioned previously (see Figure 3.2) the CBA sub-system includes one air-cored coaxial cable section. This further divided into the cable room phasing section and the underground section. It is assumed in this analysis that this type of cable is most affected by water intrusion and that the other RG-11/U type cable is not significantly affected. This is reasonable because the solid-cored dielectric of the RG-11/U limits the water collection area and the vertical placement of the cable along the antenna pole forces all water to drain to the pole base. So any water damage to this RG-11/U section will typically be limited to corrosion resulting from water travelling by capillary action around the outer sheath. No evidence of this has been found so the assumption that the Aeraxial sections alone are vulnerable to water ingress is valid.

Two approaches to determining the Aeraxial cable length using TDR techniques were apparent. First, the TDR equipment could be applied to an isolated Aeraxial section of the complete cable system. This would eliminate the effects of all other cable sections and components (i.e. patchboard, connectors, phasing cable section, etc.), enabling the characteristics of the Aeraxial section to be determined alone. Alternatively, the complete CBA sub-system could be probed in place by the TDR equipment and an estimate of the effects of the non-Aeraxial components established and removed to provide a similar estimate of the Aeraxial cable length. The latter technique was implemented here primarily because of time constraints and labour availability which precluded the use of the significantly more labour intensive technique first described. It was thought that any loss of precision in calculated cable lengths resulting from the implementation of the second technique was tolerable because the main focus of the Phase I maintenance programme was establishing working CBA sub-systems rather than precisely determining their inherent characteristics. Section 3.6 outlines a technique not dissimilar to that technique first described for use in any future CBA sub-system maintenance.

The total time between the initial and return pulse can be used to determine the cable length. Equipment system I was used (refer to Figure 3.2 on page 101) and a typical TDR trace obtained is shown in Figure 3.4 on page 111. In the simplest case,

comprising a single cable type, cable length (CL, in metres) is given as

$$CL = \frac{c \triangle t \,\mathrm{VF}}{2} \tag{3.12}$$

where c = speed of light, m/s
$\triangle t$ = pulse two-way time, in seconds
VF = velocity factor

So the equation for the round trip time ($\triangle t$) in a single cable section can be easily obtained from Equation 3.12. Considering the case for equipment system I, $\triangle t$ is the result of a pulse traversing four distinct cable sections and can be re-written as $\triangle t_{total}$ $= \triangle\ t_{3.63mcable} + \triangle\ t_{Areaxial} + \triangle\ t_{RG11/U} + \frac{1}{2}\ (\triangle t_{CROprobe})$. Hence the total time (in seconds) in a TDR measurement using equipment system I is given as

$$\triangle t_{total} = \frac{2}{c}\Big(\frac{CL_{3.63}}{VF_{3.63}} + \frac{CL_{Aeraxial}}{VF_{Aeraxial}} + \frac{CL_{RG-11/U}}{VF_{RG-11/U}} + \frac{CL_{probe}}{2VF_{probe}}\Big) \tag{3.13}$$

This can be rearranged to give the length of the Aeraxial section (CL_A) in metres as

$$CL_A = VF_A\Big(\frac{\triangle t_{total}}{2} - \frac{CL_{3.63}}{VF_{3.63}} - \frac{CL_{RG-11/U}}{VF_{RG-11/U}} - \frac{CL_{probe}}{2VF_{probe}}\Big) \tag{3.14}$$

and providing a normal distribution, an estimate of the error ($\triangle CL_A$) as

$$\triangle CL_A = CL_A\Big(\frac{\triangle VF_A}{VF_A} + \frac{\triangle(\triangle t_{total})}{\triangle t_{total}} + \frac{\triangle CL_{3.63}}{CL_{3.63}} + \frac{\triangle VF_{3.63}}{VF_{3.63}} + \frac{\triangle CL_{RG-11/U}}{CL_{RG-11/U}} + \frac{\triangle VF_{RG-11/U}}{VF_{RG-11/U}} + \frac{\triangle CL_{probe}}{CL_{probe}} + \frac{\triangle VF_{probe}}{VF_{probe}}\Big) \tag{3.15}$$

The parameter values used to calculate the Aeraxial length using the above formula are displayed in Table 3.8.

The accuracy of the electrical length or distance to a fault is dependent on the precision of each quantity in the formula applied. In all cases here the error associated with the velocity factor of the coaxial cables (and other cables) is the most significant. This is the case for most practical applications of modern TDR systems.

Equation 3.14 and Table 3.8 were used to calculate Experimental Dry (ED) cable length on all surveyed antennas in the array which exhibited no water ingress in

Parameter	Value	Estimated Error	Units
VF_A	0.79	0.0158	m/s
t_{total}	-	0.05	μs
CL_{363}	3.63	0.01	m
VF_{363}	0.66	0.006	-
CL_{11}	10.4	0.5	m
VF_{11}	0.78	0.0156	-
CL_{probe}	1.2	0.02	m
VF_{probe}	0.8	0.0198	-

Table 3.8: Parameter values used for Aeraxial cable length calculations.

the TDR trace and providing a $\triangle t_{total}$ could be obtained from the TDR trace. Similarly Experimental Wet (EW) cable length was calculated for all surveyed antennas exhibiting water ingress.

In a method similar to that described in section 6.3.1, Holdsworth determined the CBA sub-system phase difference values on 29 May 1996. The values were obtained using one hour, 2-min observations ranging from 78 to 86 km with a signal-to-noise ratio (SNR) exceeding 10 dB [*Holdsworth & Reid*, 2003]. A description [*Holdsworth*, 2001*a*, private communication] of the method used to obtain the relative CBA sub-system phase differences across the entire array is important in the interpretation of results.

Specifically, a group of central CBAs was chosen and their respective antenna phase differences were measured. A subset of these antennas that exhibited similar phase difference were interpreted as good (fault/water free) and were used individually as reference antennas in a further six antenna groups to effectively cover the complete array. Emphasis was made in locating each reference antenna in the central position of a tightly clustered group in order to maintain a high degree of correlation between adjacent CBA recorded time-series. Failure to observe this point means that significantly separated (i.e. non-clustered) antennas will be sampling different components of the ground diffraction pattern, leading to a degradation in correlation and thus misleading or unobtainable phase difference values. If the antennas selected as reference antennas

are representative of fully-functioning CBAs, those systems that contain faults, such as water ingress, may be identified by a having a significant deviation from the reference phase error value. In particular, water ingress is identified by having a significant negative phase difference. Some atmospheric phase values could not be found because of sporadic antennas exhibiting an abnormally high noise behaviour.

The relevant parameters were tabulated in an array layout diagram for all the antennas surveyed in Phase I of the antenna maintenance regime. Each CBA sub-system entry contained Antenna name, nominal original antenna wavelength, atmospheric phase error value (ϕ), Aeraxial theoretical length (T), Experimental Wet length (EW) and Experimental Dry length (ED). From these parameters two descriptors were calculated, $\Delta(EW - T)$ and $\Delta(ED - T)$. Because water in an air-cored cable will tend to increase its electrical length due to the decrease in velocity factor, $\Delta(EW - T)$ should be a large positive value if water is contained in the cable. Similarly, if all the water is excluded from the core of the cable (and no other electrical lengthening effects are present), $\Delta(ED - T)$ should be zero or a small negative or positive value as the experimental length (ED) approaches the theoretical length (T). To this a tag was added if water was found to come out of the cable while it was being forced out. This was graded into four levels; very low, low, intermediate and high. Each antenna was then cleared of any cable faults revealed after water eradication if possible. Any persistent faults were graded into major, intermediate and minor categories.

In order to validate the use of the theoretical Aeraxial cable length (T) in later calculations the complete data set was reduced to only those CBA sub-systems that exhibited no faults and no history of water. This was taken to represent a *Dry* CBA sub-system and any length calculated from TDR trace of this system would be a *Dry* value. Further, it was expected that this *Dry* cable length (ED) would be the same as T or that a difference of the two parameters, $\Delta(ED-T)$, would be distributed around zero metres. The antennas selected for this study are tabulated in Table 3.9. Shown also is the CBA sub-systems nominal wavelength, atmospheric phase error value and difference value, $\Delta(ED - T)$.

Nominal Wavelength [λ]	**Antenna**	ϕ [degrees]	**Δ(ED-T)** [metres]
0.5	6E6		-0.7
	6N6	-3	-0.7
1.0	5N6	+7	-3.9
	7E6	+8	-1.5
1.5	7E5	+5	-0.2
	5E5	+20	-6.9
2.0	4N6	-4	-2.7
	6N4	0	-1.5
2.5	5N4	-3	-2.1
	6E3		+0.2
	7E8	-5	+1.4
	8N4	-1	-2.1
	8E5	-1	+0.2
	8N5	-8	+0.2
	9E6	0	-4.5
3.0	3N5	+6	-0.4
	7N9	+7	-2.7
	9E5	+4	-2.7
	9N5	-25	+3.2
3.5	2N6	+6	-1.0
	3E9	-3	-3.3
	4E9	-3	-1.0
	6N2		-1.0
	6N10	-9	-1.0
	8E3	-5	+0.2
	8N3	-13	-1.0
	9N3	-16	-1.0
	9N4	-5	-3.3
	9N8	+15	-3.4
4.0	1N6	-3	-3.9
	2N5	+2	-1.6
	2E7	+23	-3.9
	2N8	-13	+2.0
	6E11	-28	+5.5
	6N11	0	+4.4
	7E10	-51	-1.6
	8N2	-14	-0.4
	8N10	0	+2.0
	10E5	+12	+7.9
	10N5	0	-1.6
	11E6	+17	-3.9
4.5	1E7	+6	-2.2
	2N9	+9	-4.5
	7E1	-11	-4.5
	10E9	+7	-2.2
	11E5	+12	-2.2
	11N5	-16	+7.3

Table 3.9: Calculated parameters of Cable-Balun-Antenna sub-systems not affected by water ingress. Tabulated are Nominal CBA wavelength, CBA sub-system identifier, Atmospheric phase error value (ϕ) and Δ(ED-T), the difference between the TDR derived cable dry length and the theoretically determined cable length (T). A total of 47 entries are tabulated.

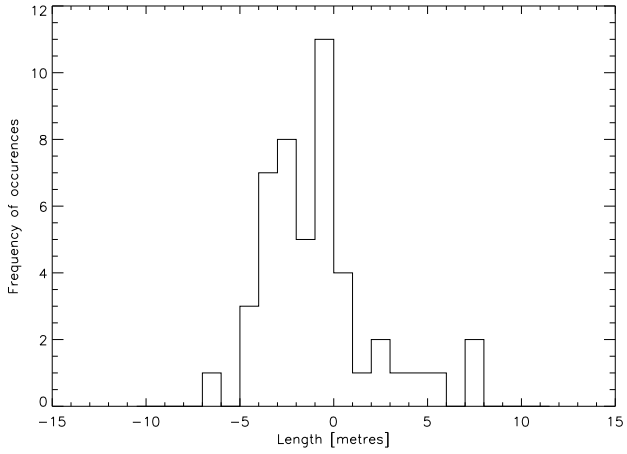

Figure 3.17: Distribution of Δ(ED-T) for the data values displayed in Table 3.9. N = 47 and the binsize is 1 m.

Figure 3.17 shows the distribution of $\Delta(ED - T)$ for the data values displayed in Table 3.9. It can be seen that the distribution appears centred around just above -2 metres. This indicates perhaps a minor over estimation of T or an underestimation of ED. Factors influencing the individual parameters used in this calculation have been mentioned previously in section 3.2.1.1. Of particular note is the peak-to-peak measurement of the time interval. This may introduce a bias into the length measurements obtained. Another factor that may influence the spread of values in the distribution is the larger set of 4.0λ values included in the sample. The errors in cable length calculations only increase as nominal wavelength increase. In fact the greater number of higher nominal wavelength values used in this distribution only serve in widening the spread of this distribution. Also the limited sample size may contribute to the slight asymmetry about zero length. However overall agreement is reasonable and it is assumed that TDR derived cable length approximates *Dry* Aeraxial cable length sans any further cable discontinuities.

As expected the atmospheric phase error values representing *Dry* CBA sub-systems are mostly distributed around zero degrees. However there are four examples lying outside a -20 $\leqslant \phi \leqslant$ +20 range. Of these, three values exceed this range by less than ten degrees and the fourth by 31 degrees. From this data it is assumed in general that phase error values of CBA sub-systems contained within -20 $\leqslant \phi \leqslant$ +20 represent a fully functioning system.

In order to determine if the exclusion of water and the subsequent repair or removal of any water hidden faults on a CBA sub-system returned the system to expected (theoretical) cable length specifications, the surveyed data set was reduced to all cable systems that contained water with those antennas having a continuing fault being excluded from the sample. If such examples were included the results would be skewed due to the increase in magnitude of $\Delta(ED-T)$ as some cable discontinuities or faults may add to the TDR time and hence ED cable length. What remained is the before and after water ingress difference length values of a fully functioning antenna system derived from TDR times using equipment system I. These are tabulated in Table 3.10.

In all cases where there are two parameters available ($\Delta(EW-T)$ and $\Delta(ED-T)$), the exclusion of water has made the experimental length converge to the theoretical length as expected. This result allows for a quick confirmation of the completed fault maintenance of water affected cables. If the distribution of $\Delta(ED-T)$ values are plotted (See Figure 3.18) it can be seen that a similar result to Figure 3.17 is obtained.

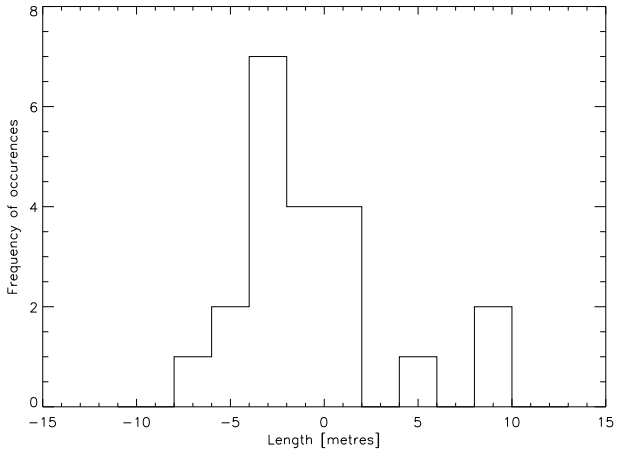

Figure 3.18: Distribution of Δ(ED-T) for the data values displayed in Table 3.10. N = 21 and the binsize is 2 m.

λ	**Antenna**	ϕ [degrees]	Δ**(EW-T)** [metres]	**Water Amount**	Δ**(ED-T)** [metres]	ξ [metres]
1.0	5E6	+11		■■■	−3·9	
	6E7	−53		■■■	−1·5	
	7N6	−36	−0·4	■		
1.5	7E7	−1	−0·9	■■		
	7N7	−3	1·4	■■■		
2.0	4E6	0	23·3	■■■	−5·1	28·4
	6E4	−1	13·9	■■■	−0·4	14·3
	6E8	+12		■■■	−3·9	
2.5	4N8	−42	12·1	■■■	−2·1	14·2
	5E8	−58		■■■	0·2	
	5N8	−37			−4·5	
	8E8	+5	−2·1	■■		
3.0	3E7	+16	14·6	■■■	−6·3	20·9
	3N7	−1	44·6	■■■■	−0·4	45·0
	5E9	−61	23·3	■■■	−2·7	26·0
	5N9	−24	20·9	■■■	−2·7	23·6
	7E3	−9		■■	5·6	
	7E9	−59	17·4	■■■	8·1	9·3
3.5	2E6	−4	5·0	■■■		
	3E8	−23	8·5	■■■		
	4E9	−3			−1·0	
	6E2	–	−3·3	■■■		
4.0	5E10	−84	22·1	■■■	−3·9	26·0
	5N10	−33	25·7	■■■■	−1·6	27·3
4.5	1N7	−6	1·4	■■■		
	3E10	+4	57·1	■■■■	1·4	55·7
	3N10	+12		■■■	−2·2	
	10E3	−132	45·2	■■■	1·4	43·8
	10N3	+126	76·0	■■■	9·7	66·3
	11N7	−3	3·8	■		

Table 3.10: Calculated parameters of Cable-Balun-Antenna sub-systems before and after water ingress. Tabulated are CBA sub-system nominal wavelength (λ), CBA identifier (Antenna), Atmospheric phase error value (ϕ), difference between TDR length with water ingress and theoretical cable length (Δ(EW-T)). The level (Water Amount) of water found in the Aeraxial section was graded as very low (■), low (■■), intermediate (■■■) and high (■■■■). The difference between the TDR derived cable length after water exclusion and the theoretical cable length (Δ(ED-T)) is followed by (ξ), the difference of the two descriptors Δ(EW-T) and Δ(ED-T). A blank entry represents no data value available. A total of 30 entries are displayed. Antennas tabulated were confirmed clear of all faults after water eradication (hence no extra effects on TDR time).

Missing data values are mostly attributed to low quality TDR traces precluding accurate time interval measurements. This distribution has a similar form to the previous dry cable length distribution except for some outliers. Here, the smaller size of this ensemble will have a significant effect on the form of the distribution in a more marked fashion that the previous distribution.

Note that this set will include those CBA sub-systems where later repaired cable faults initially contributed with the water to increase a cables length. In such cases the calculated EW parameter is thus not solely due to the effect of water ingress in the cable, however it is postulated that this situation will affect only a limited number of cables to a small degree.

It was also hypothesized that the difference (ξ) between $\Delta(EW-T)$ and $\Delta(ED-T)$ will be correlated with the Water Amount. Here large values of ξ, representing a significant change in cable length value post water eradication, should be correlated with significant levels of water found during the water extrication process. While it can be seen that intermediate and high levels of water amount appear to be correlated mostly with larger ξ values, the limited number of observations precludes any decisive judgement to be made. The observations that are tabled unfortunately omit any data points for low and very low water levels, resulting in a much narrower picture of the situation than would have otherwise been presented. However, there are more significant concerns with such an analysis of water level. For instance, measuring water in the current survey was a (qualitative) best estimate on site whereas a (quantitative) volumetric analysis of water extricated would have perhaps been more informative. Also, any subsequent analysis must account for the fact that longer wavelength cables have an increased volume for storage of water compared to shorter cables and this will be borne out in the data. It should be noted that a more detailed analysis of water level requires significantly more time spent on each CBA sub-system, which was not commensurate with Maintenance Phase I aims at the time.

At what level does water in the cables become an influence on cable VF, impedance and ultimately cable electrical length? For instance, very low levels of water may not

have a noticeable influence on the VF or impedance to significantly affect electrical cable length probed using the current equipment. In this situation the tabulated values signifying very low water levels antennas may not be expected to be correlated with significant atmospheric phase values. This question can perhaps be better addressed using a more capable equipment system.

On the question of does a larger negative atmospherically derived phase error value ($\phi \leqslant$ -20°) translate to water in cable, the data does not seem to bear this out. Data in Table 3.10 shows that large positive atmospheric values are approximately equally likely to be correlated with the presence of water.

More telling is perhaps the results of 6E4, 3N7 and 3E10, where a small phase error value was correlated with a significant water level being found. This is contrary to the expected behaviour and may indicate the unsuitability of these two data sets being compared. Further reason for this assertion lies in the two year period between the atmospheric data set and the water level determined in the Phase I maintenance period. This substantial elapse of time may have affected the volume and location of water within the cables, rendering a direct comparison problematical at best. Variation in local environmental conditions such as temperature or water drainage may have a significant effect on the water level contained in the cables or influence water migration. Such behaviour is more likely to occur if there is some breach in cable integrity that allows the transfer of moisture directly. Specific behaviour of the water level according to these factors is at present unknown however the completely static behaviour of the water over such a period is considered unlikely. This concern can be dealt with in the future by the obtaining the atmospheric phase values for the complete array in the days immediately preceding any extended maintenance period. This should result in any water variations being sufficiently minimized.

An alternate view of this data could be obtained if it is assumed that the all positive ϕ values contain a *wrap around* error in that they have exceeded -180°. If these are corrected and thus all positive values are viewed as large negative values it appears

that the atmospheric phase error values conclusively describe water affected CBA sub-systems. Supporting evidence may be found in the water level recorded for each of these corrected phase values. In this case, it would be expected that a phase value exceeding -180° would be correlated with a higher than average water level. The table shows that this is the case, where water level is intermediate to high in all instances bar 8E8 where a low water level was recorded. Further to this analysis it may mean that some low negative values indicate extremely high water levels due to a 2π wrap around. This would explain 3N7 and 5N10. If this approach to the interpretation of the atmospheric phase error values is deemed valid it places emphasis on the recorded water amount as a valuable confirmation aid of the technique. This perhaps suggests future controlled studies into the phase behaviour of the Aeraxial cable under varying amounts of water ingress.

Vital to this technique is the initial choice of reference antennas used in the atmospheric phase error value calculation. In the current analysis it has been assumed that these reference antennas are in fact performing at their optimum. If some were in fact atypical CBA sub-system examples, the atmospheric phase error value distribution would be at the least, less coherently distributed. In this case it would be expected that optimum CBA sub-systems were clustered around non-zero atmospheric phase values. Perhaps subsequent choice of these reference antennas could involve the use TDR and other methods to establish if each reference antenna system is in fact fault free. Another consideration, albeit a minor one, is that the atmospheric conditions used to obtain the phase error values are not abnormal. If significant atmospheric return is distributed off zenith this will have a detrimental effect on the phase values obtained.

While it has been assumed in this analysis that the dominant causes of electrical length variation are water contained in the air-cored dielectric and significant discontinuities along the cable length, they are not the only causes of electrical cable length variation. Electrical length variation with temperature also has been studied [*Clements*, 1972], but this effect is estimated to be small (i.e. $\ll 1$ m) for the

daytime temperature ranges experienced during the measurements (both TDR and atmospheric) at the BP field site.

If water ingress has occurred in a CBA sub-system, it is likely to also manifest as abnormal complex impedance readings obtained using the VIM. However, such values were not included for any correlation analysis at this time because MF antenna array complex impedances are difficult to interpret *sans* water ingress. Impedance measurements of MF antenna arrays are often observed to varying seemingly unpredictably [*Brown*, 1992]. Patchboard measured complex impedance probes the complete CBA sub-system and as such is influenced by the behaviour of each component in the system. This is further complicated by the variability of each component's characteristics, many of whom each appear to have dependencies including, but not limited to, weather (incorporating season, temperature, wind speed, precipitation), water drainage, soil moisture and conductivity. The result of this situation is that specific affects on complex impedance caused by water ingress are difficult to separate from the combination of other listed effects. Until further research *in situ* is carried out in separating specific causes and effects, complex impedances are best used as a coarse measurement of antenna fitness[12].

3.3.4 Coaxial cable electrical length using equipment system II

Accurate estimation of coaxial cable length has potential applications more far reaching than only confirming the operational status of CBA sub-systems. In order to isolate the specific nature and cause of cable faults along cable sections, cable length calculations can be used to determine fault location in the field. Geographically precise fault location obtained from high resolution TDR equipment can dramatically reduce the maintenance time and labour expended in pursuit of these faults. It was expected that such techniques applied to CBA sub-systems would provide definitive data on the root cause(s) of serious cable faults identified in Maintenance Phase I survey that were

[12]A programme of regular sampling of patchboard complex impedances has been instituted with a view to future analysis. Correlation with data from the adjacently located Automatic Weather Station may yield the required answers.

primarily responsible for 42.55% of the MF antenna array classified as *Not operational* and *Operational, with fault(s).* This investigation is described in the following section.

The ensuing years since array installation has seen a number of underground cable sections develop serious faults. Subsequently, these CBA sub-systems have not been used in transmission or reception configurations. This has reduced array flexibility in terms of the individual CBA sub-systems available for use in radar beam pattern configurations. Recently, the survey outlined in section 3.3.2 using TDR techniques and equipment system I has confirmed these existing buried cable faults as well as identifying others. Previous TDR systems, used infrequently to monitor the array status, have suffered from poor resolution to clearly identify single cable faults. Also, the manual location of a single buried cable in a cable bundle in the field was time-consuming without dedicated cable location equipment, as was the excavation work necessary to unearth the desired cable section for examination. It was envisaged that any new TDR equipment system and technique configured for fault location would address these points. Relevant suggested improvements to the TDR equipment system I (see section 3.2.1.1) were incorporated in equipment system II (described previously in section 3.2.2). The location of buried cables in the field was addressed by the trialling of commercially available cable location equipment.

In order to evaluate a possible fault location method, a CBA sub-system with long standing faults along the buried cable section was chosen (e.g. 6E5). During Maintenance Phase I, this CBA sub-system was prepared for major field fault location by the removal of minor problems along its length. All water was extricated from the dielectric and a small section of heavily corroded cable in the cable phasing room was removed. Further corrosion was removed using a chemical treatment, but it is likely that some corrosion of the ground shield remains intact underneath the cable's outer jacket. At the conclusion of this preliminary work, CBA sub-system 6E5 had TDR traces taken using equipment system I which indicated two main discontinuities existed along its cable length. The TDR trace recorded from this time is shown in the Figure 3.19. Two discontinuities can be observed, between the initial pulse and

the return from the balun. From a TDR trace taken prior to this preliminary maintenance Δt was measured to be 1.17 μs, giving an Aeraxial cable length of 123.1 m. This compares poorly with the theoretical Aeraxial cable length of 109.2 m expected for a 1 λ nominal wavelength cable section but the difference can be attributed to the discontinuities present in the cable and the water found. After the preliminary maintenance procedures outlined above the measured Aeraxial cable length was 117.2 m (Δt = 1.12 μs). Although two discontinuities can be distinguished in this figure, it is difficult to extract any specific information about the fault type or location. This is a direct result of the resolution capability of the equipment system I. Equipment system II was used in order to ascertain more information on this cable system.

Figure 3.20 shows the TDR trace recorded using the higher resolution equipment system II during Maintenance Phase II with a pulse width of 8 ns. Note that this reduction in pulse width has led to better discrimination of adjacent faults compared to the 210 ns pulse width used to obtain Figure 3.19. The two major discontinuities of the previous figure can now be more clearly resolved along with two minor discontinuities adjacent to the initial pulse due to the equipment feeder cable configuration. The large negative spike located near the centre of the figure is due to the short inserted at the end of the Aeraxial cable. The low amplitude re-reflection of the faults on the right of the figure can be ignored.

A new estimate for Aeraxial cable length can be determined from the time interval measurement (Δt = 1.085 μs) of this figure and using Equation 3.14 after omitting terms not representative of equipment system II. The resulting Aeraxial cable length is 124.1 m. This is significantly longer than the theoretical value of 109 m tabulated in Table 3.7 but could be attributed to the deleterious effect on TDR time (Δt) the multiple cable discontinuities have and highlights the effect of serious faults on cable propagation characteristics.

The form of the discontinuity displayed in this figure can give some indication of the nature of the fault. Here the first major discontinuity may be join or splice, while the second major discontinuity appears to be a short due to its similar form to the

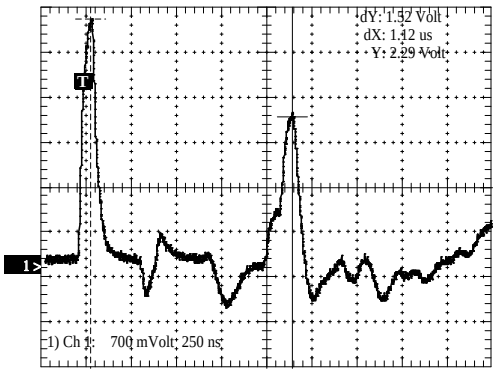

Figure 3.19: TDR trace of 6E5 using equipment system I (refer to Figure 3.2) on 29.5.98. This system probes the complete CBA sub-system (i.e. no short introduced at antenna pole base). The figure shows voltage (700 mV/div) against time (250 ns/div) with mark T indicating the DSO trigger point. The two vertical lines and cursor positions are placed on the peak of the initial (dashed) and return (solid) pulse. The respective differences in cursor position dY and dX are shown in the upper right of the figure and are 1.52 Volts and 1.12 μs seconds respectively. The trace shows two discontinuities between the initial and return pulse. Equipment system I allows general indication of the presence of discontinuities, however their specific nature and position are difficult to resolve due to the limited capabilities of this system. The signal to the right of the return pulse can be ignored.

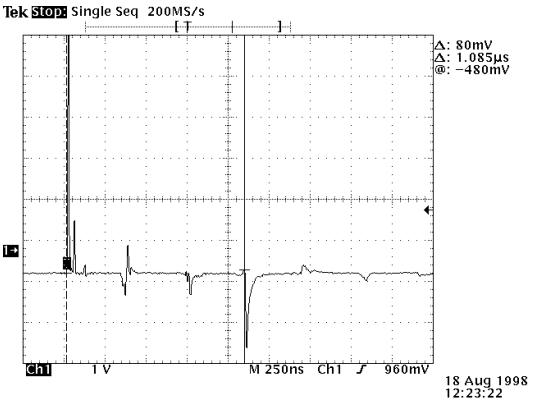

Figure 3.20: TDR trace of 6E5 using equipment system II on 18.8.98: Overview. Displays voltage (1 V/div) versus time (250 ns/div). Unlike Figure 3.19, a short had been introduced at the end of the Aeraxial cable (pole base) producing the large negative spike in the centre of the figure. Looking along the trace from left to right, the initial pulse is followed by two decreasing amplitude features resulting from the connecting system of the test equipment. The next two returns are the discontinuities observed in the previous diagram which can now be more clearly resolved. Again the cursor is positioned at the beginning of the initial (dashed) and return (solid) pulse. The time difference (Δ) between these two points is displayed in the upper right of the figure and is 1.085 μs. This time can be used in an estimate of the Aeraxial cable length.

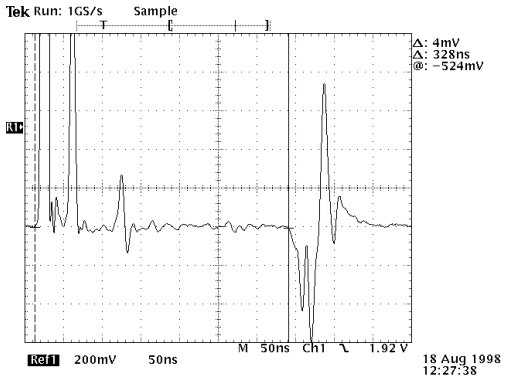

Figure 3.21: TDR trace of 6E5 using equipment II on 18.8.98: Focus on first discontinuity. Displays the voltage (200 mV/div) versus time (50 ns/div). The cursor is placed at the start of the initial pulse (dashed) and at the return from the discontinuity (solid). The time difference (Δt) is 328 ns.

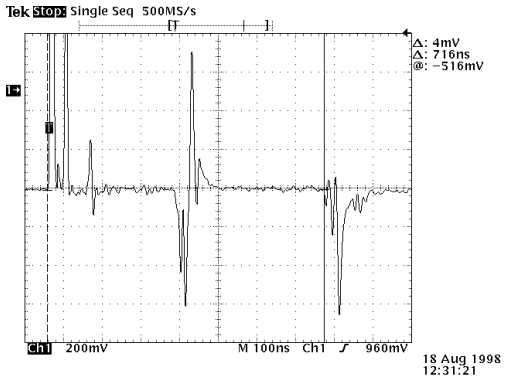

Figure 3.22: TDR trace of 6E5 using equipment II on 18.8.98: Focus on second discontinuity. Displays the voltage (200 mV/div) versus time (100 ns/div). The cursor is place at the start of the initial pulse (dashed) and at the return form the discontinuity (solid). The time difference (Δt) is 716 ns.

short inserted at the end of the cable.

Figure 3.21 displays an expansion of the time axis in order to focus in on the first major discontinuity, while Figure 3.22 focuses on the second. Using the temporal intervals noted in the figures the distance to the first and second discontinuity are 34.5 m and 80.4 m respectively. This gives a distance from the antenna patchboard and incorporates any cable phasing section in the cable phasing room for that CBA sub-system. Spot cable bundle positions were made along the west cable run at ground level to assist in accurate measurement over the terrain to the designated fault location. The commercial cable location equipment (refer to section 3.2.2 on page 115) was used to ascertain the cable bundle position at the TDR suggested fault location. A section around the suggested location was carefully excavated to reveal the west cable bundle. Further use of the cable location equipment identified the 6E5 Aeraxial cable of interest. A length along this cable was excavated but no fault could be identified. It was thought that the suggested second discontinuity location measurement would be adversely affected by the effect of the first discontinuity and no time was allocated

to tracking this particular fault.

A similar technique was used to identify a significant discontinuity along the buried section of 6N5, but similarly the tell tale physical evidence of a sheath breach could not be found. Some further work to identify if the faults in the other cables of the west cable bundle occurred at similar TDR locations was undertaken without finding a distinct correlation. As a significant increase in operational CBA sub-systems had been achieved to this point and further focused maintenance work in this area would translate to a much smaller number of antennas achieving operational status in an allotted time, it was thought prudent to halt CBA sub-system maintenance to direct future time and labour to maintenance of the transmitter system.

A premise of the technique used is that an electrical fault is associated with a visible mechanical fault along the cable such as a deteriorating outer sheath etc. While this assumption has validity it may not always be the case. For instance, water ingress may have damaged the dielectric from the interior of the cable such that an electrical fault exists but damage has not yet translated to the cable's outer sheath.

In terms of addressing faults sequentially, *Moffitt* [1966] suggests that it is best practice to address discontinuities or faults from the input end outwards where each return is either repaired or isolated before attention progresses to the next. Factors influencing this recommended approach include the degrading pulse risetime with each discontinuity, the increasing pulse distortion with cable length due to cable characteristics and obscuring pulse re-reflections.

It is apparent that further work could be undertaken in the tracking of these underground cable section faults at some later stage and an approach to such work is outlined in section 3.6.

3.4 Analysis

An analysis of the data presented in the previous section is outlined with a view to isolate the causes of faults encountered throughout the antenna array system. A discussion of components of the CBA sub-system is ordered corresponding to the present occurrence of faults, being Cable (54.86%), Balun (13.19%) and Antenna (4.17%). Conclusions from this analysis are made in the context of the objectives of the previous 1992/94 array upgrade and with a view to future maintenance concerns of the array.

Water intrusion into the air-cored dielectric has been an often encountered problem of the MF array over the decades of operation and the current survey results place it as the major cause of CBA sub-system faults. Efforts to stem the intrusion of water into the underground sections of Aeraxial cable were undertaken during the 1992/94 array upgrade. The installation of a PCB mounted balun circuit inside a waterproof UV-stabilised plastic balun box has substantially prevented water collecting in the balun box[13] and replacement of the upright Aeraxial cable with solid-cored dielectric RG-11/U has apparently blocked water entering into the underground air-cored dielectric Aeraxial via this route. The mechanical fatigue problem (brought on by the water, oxygen, corrosion cycle and perhaps the Aeraxial's non-UV stabilised outer sheath) of the upright section of coaxial cable encountered previously (see *Vandepeer* [1993]) has also been addressed by these two improvements. However, data presented in section 3.3.2 clearly shows the extent of the presence of water in the underground Aeraxial cable. What is the main mechanism by which this water ingress occurs?

To enable further interpretation of the data in terms of locating responsible water ingress mechanisms, a schematic plan of the entire array was produced highlighting the detection of water and its position within the array for all surveyed antennas during the current study. Figure 3.23 displays the result of this. Here, the water volume found

[13]Small holes in the base of the balun housing, necessary for the drainage of condensation formed within the balun box, do provide an access point for water ingress but the level of water damage from this entry point has been found to be negligible.

in any buried Aeraxial cable section of a CBA sub-system is classified into four discrete levels. CBA sub-systems not surveyed and those found to be free of water are also indicated. As mentioned previously, each *patchboard* contained 89 dipoles. Of these, 60 CBA sub-systems per patchboard were examined in the survey constituting ∼67% of each patchboard. This represents a significant proportion of each patchboard's total connected CBA sub-systems and it is assumed that the size of this sample allows some conclusions to be drawn from the data presented. However, it should be reiterated that those CBA sub-systems selected for inclusion in the survey were not randomly chosen and in fact mostly contained known fault(s) of some kind. Although this selection process was a direct result of the objective of the Phase I maintenance programme (i.e. repair antennas), it does not constitute a random sample of the entire array. Nevertheless, a substantial amount of the array was covered. This fact, together with the sampling of both north and south oriented dipole CBA sub-systems, which often resulted in many non-fault antennas being included in the survey, allows conclusions to be drawn on the distribution of the data and its applicability to array performance as a whole. It should be noted that only a significant percentage of the south-west CBA sub-systems were excluded from the survey due to their apparent operation within specification at the commencement of the survey. It is expected that this exclusion has no significant bearing on the analysis of fault mechanisms outlined here.

It is apparent from this figure that the CBA sub-systems confined roughly to the south-east quadrant are over-represented in both patchboard schematic diagrams. A characteristic of this south-east clustering of CBA sub-systems is a prevalence of intermediate to high water volumes measured. This characteristic is not borne out in most other parts of the array, where a very low to low water level is often found in water affected CBA sub-systems. Also there appears to be a possible sub-grouping of water affected CBA sub-systems located throughout the north-east of the *East* patchboard and the east and outer north-east perimeter of the *North* patchboard.

In an effort to isolate the specific cause(s) of water intrusion, all CBA sub-systems

with confirmed water problems were plotted in Figure 3.24 according to their underground trench positions. This was done to see if the water affected underground cable sections corresponded to any particular cable trench grouping or any particular geographic area. It was thought that any displayed cable grouping may indicate a localized point of damage affecting all adjacent cables while the geographic information may shed light on whether the affected cable or group of cables was located in known poor water drainage areas such as in the river bed, local water course or a known burrowing animal activity area.

Isolation of a particular point of damage that has affected adjacent cables is difficult from this diagram. Other than identifying that the east and south-east cable bundles may have such a localized point of damage due to the large number of adjacent water affected cables, its particular location(s) is not discernible from this figure. This is because water found in a cable is attributed to the entire length of the cable in this diagram. This is necessary because no specific information on actual water location within a cable section can be reliably gleaned from the TDR traces of equipment system I. Also, water may pool in a section of cable that is spatially removed from any actual break in the cable sheath. This occurs due to small variations in cable burial depth along the cable length, where locally depressed sections provide a *pocket* for water containment.

In terms of the geographic distribution of water affected cables, while many of these water affected CBA sub-systems were mostly grouped in the east and south-east sections of the array, this did not correspond to the lowest lying part of the array or a location where small animal activity was above average. This indicated perhaps other contributing factors as a cause of water ingress. In contrast to this situation is the small number of very low to low water volume affected cable sections of the north-east quadrant that do correspond to a local minimum in the terrain underneath the array [*Reid*, 1984]. This topographic depression may be considered a contributing factor to the these water ingress problems. Likely mechanisms leading to water ingress are now discussed in turn more closely to gain some perspective on the information

presented in Figures 3.23 and 3.24.

Deterioration of the cable sheath underground due to its contact with moisture and chemicals contained in the surrounding earth of this coastal (salt laden) environment is a possible mechanism for cable water ingress. This breaching of the cable's outer jacket allows moisture and chemical action to act on the woven braid of the outer shield and thin wall of the air-cored dielectric. If the air-cored dielectric wall is penetrated, water may accumulate along the length of the cavity offered by the air-cored dielectric. Seasonal fluctuations in the water volume contained in such a cable section may be observed as heavy local precipitation during the winter season, followed by dry summer periods exerts some influence on the water level contained in such buried cable sections.

The activity of local vermin and native animals (e.g. *Rattus rattus* (Black Rat), *Oryctolagus cuniculus* (European Rabbit) and *Trachydosaurus rugosus* (Shingleback Lizard), [*Strahan*, 1992; *Ehmann*, 1992]) may provide an alternate mechanism to the weathering action described above. The European Rabbit has been active around the array site and has excavated warrens around the buried cable sections. These animals may not have the jaws and teeth powerful enough to cause significant damage to a cable outer jacket but the Black Rats and Shingleback Lizards that scavenge or later occupy vacated burrows have the capacity to do so [*Morrison*, 1981]. This mechanism has a similar effect to that described above in that as soon as the dielectric wall is breached, a water entry point is provided, with the hardened burrow providing a channel for water during winter. Serious cable shorts etc., may also be achieved in this fashion. While there appears to be vermin activity throughout the array area, it is not any more prevalent in the south-east quadrant.

Other possible points for water entry are present in the connection between the termination of the underground Aeraxial section and the beginning of the upright RG-11/U section. These connection points are sealed with electrical tape and angled to minimize water entry but nevertheless provide a direct entry point into the air-cored dielectric. Again, precipitation during winter may regulate the water volumes contained in any one cable section via this possible water entry point. Similarly, the

insertion of a number of cable connectors in the field have provided another type of possible water entry point. These have been used to eliminate long standing cable faults in the past but unfortunately may also allow water entry into the air-cored dielectric when subjected to the surrounding moisture laden earth. A small number of these connectors have been used but generally don't correspond to any particular quadrant of the array.

Finally, it should be noted that the employment of an air compressor to force water from the underground cable sections in the past may not have been as effective as once thought. During the 1992/94 upgrade *Vandepeer* [1993] notes that compressed air was used and had been used prior to this upgrade period to solve this problem. It has been found subsequently that faults existed in this compressed air system that may have led to it under performing in its task, at least during this recent upgrade period. Firstly it was found that the work performed when the compressed air was released into the air-cored dielectric was significantly below specification of the air compressor. This translates to a limited amount of force exerted on the volume of water within the underground cable section and may result in water being moved from one section of a cable to another but not be completely expelled as desired. The possible occurrence of this effect has been noted [*Ludborzs*, 1996]. Secondly, moisture condensed from the air during the process of cooling by the compressor needs to be adequately removed. If not, this moisture can be transferred to the connected underground cable section. It was found that this moisture separation component was not effective in the compression of air process and may be a cause of small levels of water being added to the cable section. Reconditioning of the air compressor, replacement of the sub-micron filter and connecting hosing has seen dramatic improvements in water eradication by this compressed-air method. It should also be noted that normal condensation of water vapour within the air-cored dielectric may also cause very low traces of water to be found in some cable sections but at levels far removed from that uncovered in the south-east quadrant. Appendix E outlines a calculation of the expected water levels due to condensation alone.

Viewed together, these considerations do not sufficiently explain the extent of bias towards the south-east quadrant that the current survey results indicate. The points mentioned above may explain many of the non-clustered water affected cables but do not fully address the south-east predominance of water ingress because 1) water affected cables should occur equally across the array aside from a possible expected bias towards the watercourse lying in the upper north-east of the array, 2) vermin activity is not isolated to the south-east quadrant and occurs in clusters all around the 1 km aperture of the array, 3) the insertion of foreign cable sections or connectors to alleviate faults in the field have been used only occasionally over the arrays history and are not confined to the south-east quadrant and 4) air-compressor or condensation problems alone do not account for the volume of water found in many cables.

A study of the antenna array maintenance records provided a different perspective on the this apparent south-east bias. Records show that a section of the array encompassing most of the south-east quadrant had its balun boxes upgraded during 1992/93. This section was the first to be upgraded to the current standard of balun, feeder, dipole and upright cable to facilitate transmission and reception on the large array. Of the thirty antennas upgraded, only six had a TDR trace taken and interpreted at this time. Recollections of this section's upgrade (e.g. *Rutherford* [1996, private communication] and *Holdsworth* [2001*b*, private communication]) indicate that less time was allotted to TDR techniques in the pressing need for upgraded and operational CBA sub-systems. Thus water already existing in the underground section of cable that entered via the original water susceptible balun box and was channelled into the underground Aeraxial section via the upright Aeraxial section may have been effectively sealed in during the 1992/94 upgrade. TDR of the underground cable section pre-balun upgrade may have indicated existing water in many of the buried Aeraxial sections. It appears TDR was initiated on a more systematic basis after these initial 30 antennas were upgraded. This initial upgraded section is outlined (solid) in *Vandepeer* [1993, Figure 4.1]. While this explanation adequately addresses the apparent south-east bias shown in the survey results, it has no bearing on adequately explaining

the non-south-east quadrant water ingress. Because of the different character of non-south-east water affected cables (that of having very low to low water levels) and with the knowledge that the water eradication process subsequent to the thirty selected antennas was improved by the more thorough use of TDR methods for instance, the source of this water ingress lies elsewhere. It is expected that these cable sections are resulting from one of the individual mechanisms cited previously or a combination of them. In particular the depressed terrain overlapping the north-east cable sections may exacerbate any cable breaching problems.

If this explanation is the case and many of the water affected cables within the south-east quadrant of the array are due to sealed water ingress at the time of the upgrade then once the water has been expelled, most, if not all cables should remain water free in the absence of other cable integrity breaches. This means that the upgrade procedures to stop water ingress may have succeeded generally, even though the current survey results indicate water ingress as the most significant problem. This can be tested by repeating the TDR tests for water ingress. Following this, perhaps a better indication of the extent of water ingress problems post upgrade may be established by subtracting the thirty south-east quadrant water affected cables from both patchboard CBA sub-systems. This results in water ingress being viewed as a significantly reduced current maintenance problem of the array.

Any water contained in cable sections can have a significant effect on the data collected using them. The consequences of using water affected cable vary according to whether transmission or reception is required. If a number of water affected CBA sub-systems are used in a particular transmission configuration, likely consequences will be a wider beam width and variations in bore-sight other than those modelled. This may be tolerable depending on the specific atmospheric observation application. Much less tolerable is the situation upon reception. If water affected CBA sub-systems are used for reception where phase information is critical in parameter calculations, such as for Angle-of-Arrival (AoA) calculations etc., significant errors will result. This aspect should be a consideration in future maintenance efforts.

Until the 1992/94 upgrade, balun problems had contributed to somewhere near 50% of CBA sub-system failures [*Vandepeer*, 1993] due to poor sealing, inadequately mounted components and poorly selected components. Currently, the balun accounts for 13.19% of CBA sub-system faults, representing a significant reduction in fault occurrences. Faults are now primarily caused by tuning capacitor malfunctions and dipole feeder failures, but it appears that all other previous balun faults [*Vandepeer*, 1993, pg 62, 63] have been rectified or dramatically reduced by the new balun design. The current survey results indicate that during the studies for an upgraded balun design in 1992 it was prudent to seek a circuit that omits tuning capacitors due to their significant effect on balun performance when malfunctioning. Any future balun design revisions should also seek alternatives to the current tuning capacitor arrangement if possible in an effort to further reduce maintenance time expended. While currently a minor cause of balun faults, the failure of the feeder connecting balun to one section of the dipole is mostly caused by the development of dry points in the electrical/mechanical connection. This occurs over time as a consequence of the connection being exposed to the harsh coastal environment despite the efforts to seal soldered joints with waterproof self-polymerising tape. Aside from the continual re-evaluation of the connection technique and materials used it is difficult to offer improvements to this connection that don't adversely affect the dipole and balun impedances.

Further analysis of the TDR traces reveals a possible area for improvement in relation to balun operation that is not revealed in the survey fault statistics. Figure 3.4 shows a typical TDR trace from a fault free CBA sub-system. All fault free CBA sub-systems display a similar TDR trace, with the only significant variations in the time delay (due to different nominal cable wavelengths) and amplitude of the return pulse. It is this variation in amplitude of the return pulse that may be optimized by a different balun tuning procedure. In an ideally matched system all transmitted pulse power will be absorbed by the balun to be radiated by the connected dipole. However the inherent variable nature of dipole impedance in forever changing environmental conditions will

create a degree of mismatch even if the balun has been tuned to theoretically predicted values. The concern is that the dipole impedance fluctuates around this theoretical value over the course of a year and a balun re-tuning at any point in time is likely to not take this fluctuation into account using the current tuning procedure.

The balun tuning technique involves the measurement of complex impedance at the balun cable input or at the patchboard, while the arrangement and value of the silvered mica tuning capacitors are varied on their pads within the balun. The primary aim is to settle on a capacitor arrangement that achieves 75 Ω $\angle 0°$. In practice it is difficult to achieve this nominal value and it is deemed more appropriate to allow some impedance magnitude variation but stringently pursue little phase variation. However, because the dipole remains part of the circuit while this tuning takes places means that the balun is tuned to match the dipoles impedance and phase at that particular moment in time. If tuning is repeated at another time it is likely that the dipoles behaviour will have changed[14]. If a 28 Ω load is substituted for the dipole during balun tuning instead of it taking place with the dipole connected a better match could be attained year round, providing that 28 Ω best represents a dipole's, year round, fluctuating impedance.

Actual dipole failures contribute only a small fraction (2.78%) of total array maintenance (CBA) concerns. Primarily, a dipole suffers mechanical failure generally brought on by corrosion or fatigue at a single point along its length. A new dipole is fashioned from the hard-drawn 2 mm diameter copper wire as a replacement. Similarly, the PVC encased fibreglass yarn or *Debeglass wire* that acts as an insulator and spacer between adjacent dipoles has required little attention in the past decade, though a visible degradation its UV stabilised jacket material has been observed, which contributes to eventual spacer failures. However it appears that the use of more appropriate materials for the antenna system on the whole has resulted in fewer dipole (and associated

[14]Impedance variations can be caused by changing water table level, rain etc.

system) problems in the intervening years. In fact, many of the upgrades have successfully alleviated MF antenna array problems and facilitate the array for continued use into the 21st century as Vandepeer states.

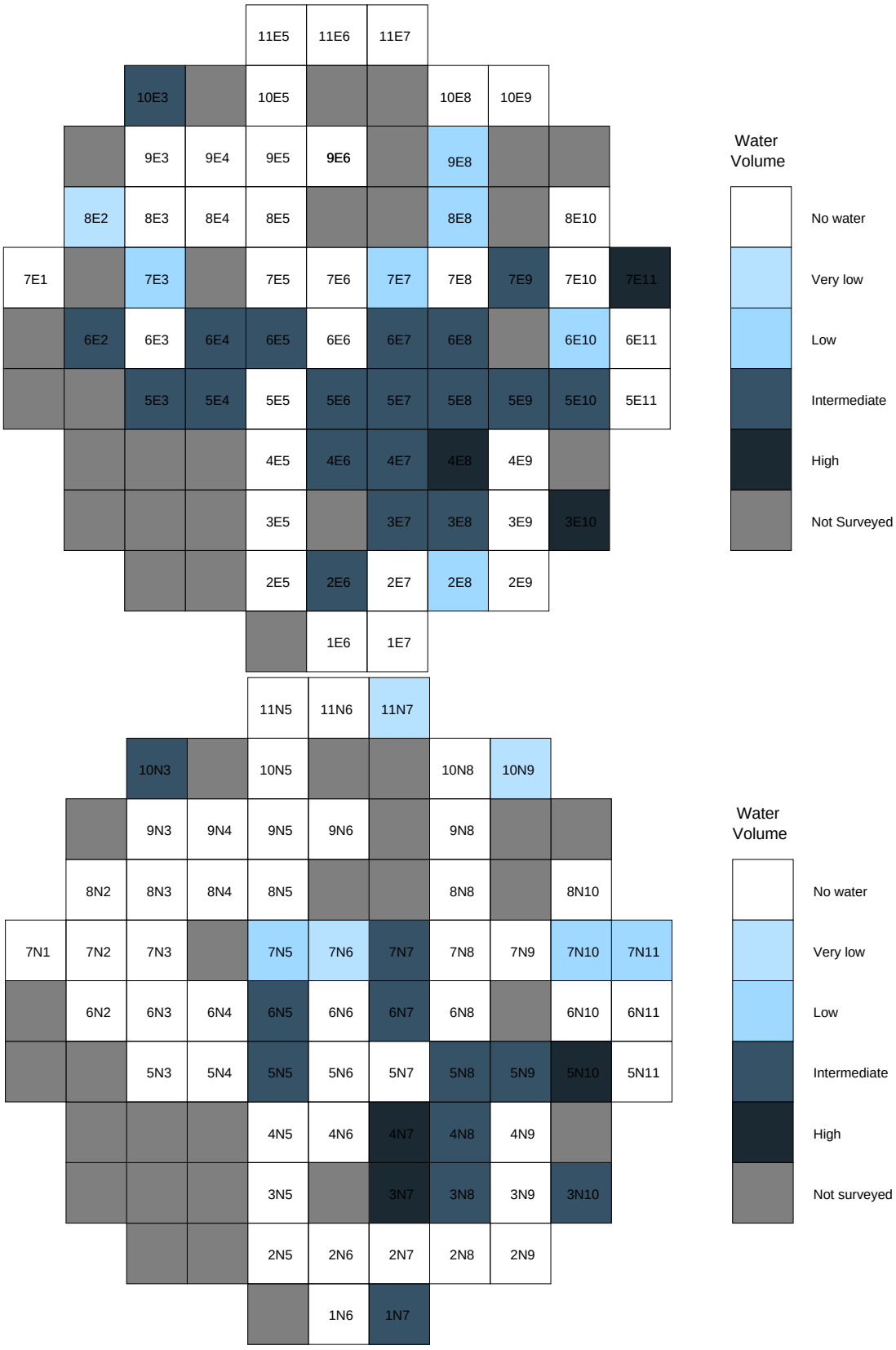

Figure 3.23: Array location and water level found in the underground cable section of the *East* (Upper diagram) and *North* (Lower diagram) patchboard Cable-Balun-Antenna sub-systems during the Phase I maintenance period.

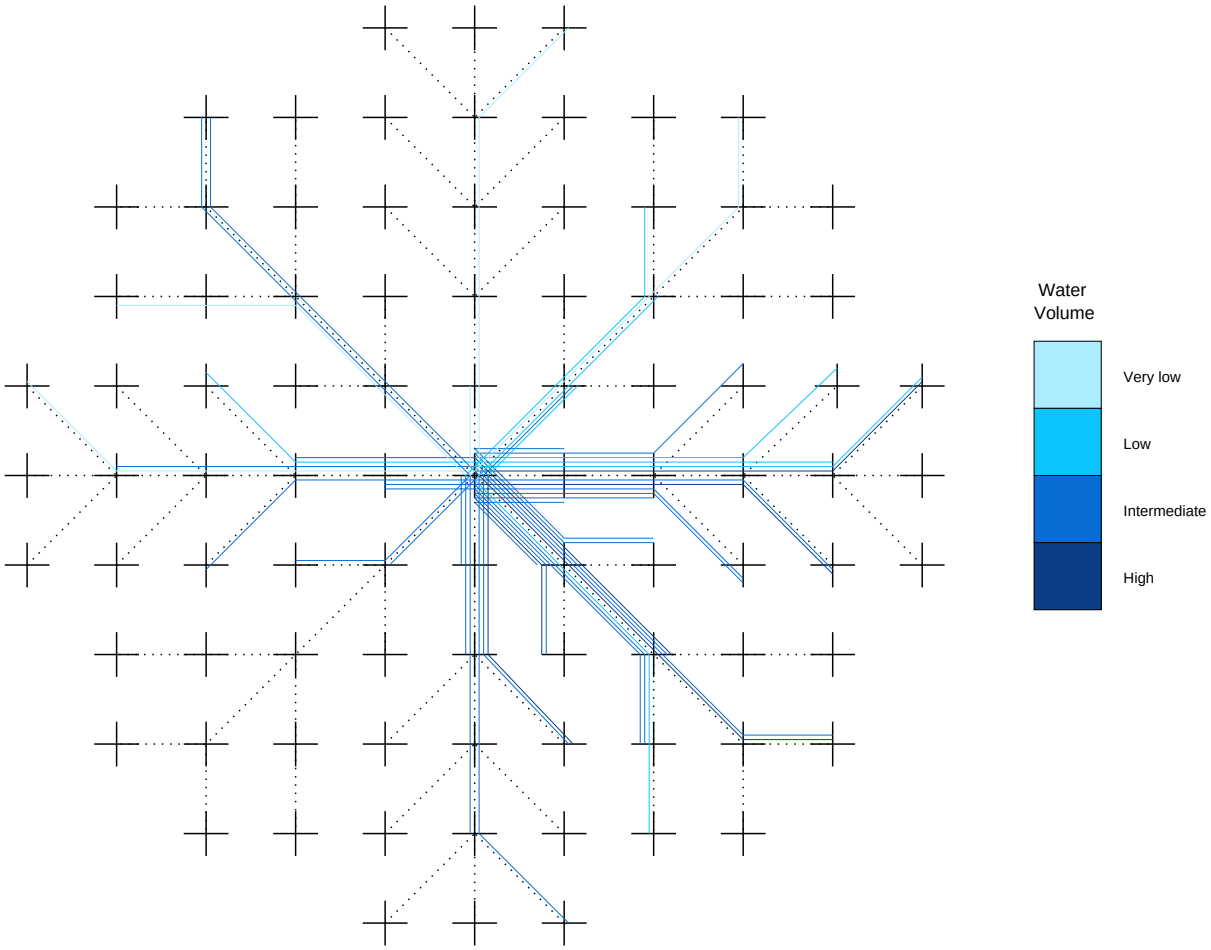

Figure 3.24: Distribution of water affected cables according to their underground trench layout (dotted). The volume of water found in each cable is indicated.

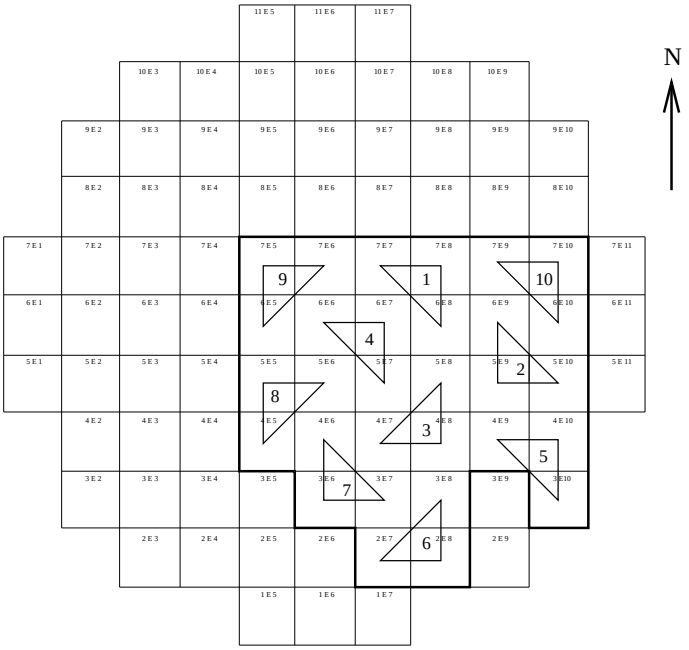

Figure 3.25: The first thirty refurbished antennas of the 1992/94 upgrade period (from *Vandepeer* [1993, Figure 4.1]). The outer (solid) line indicates the region containing the thirty upgraded antennas and the triangles indicate ten antenna groups configured from these antennas for an initial data collection period. Note that although this diagram highlights only those antennas on the *East* patchboard all of the corresponding antennas on the *North* patchboard were upgraded at the same time.

3.5 Summary

A comprehensive maintenance programme for the MF antenna array was devised and implemented to maximise the array operational status. A significant increase in the number of Cable-Balun-Antenna sub-systems available for transmission and reception was achieved. An overview of faults encountered during the current maintenance period was detailed and comments were made on their source as either stemming from design deficiencies or from expected component attrition within a progressively ageing array. Various time domain reflectometry equipment systems were assembled and applied to the particular requirements of the separate phases of antenna array maintenance with equipment system I providing immediate feedback of CBA sub-system status at a limited resolution while equipment system II allowed more interactive assessment of particular cable faults in the field due to its higher resolution. When allied with established maintenance techniques, TDR dramatically increases the effectiveness of CBA sub-system maintenance.

Investigations into Aeraxial coaxial cable velocity factor and risetime are in reasonable agreement with previously utilised values. Coaxial cable electrical lengths derived from theory and found via experiment have been utilised in the development of a measurement technique that can identify water affected cables. Also examined was the correlation between atmospherically derived system phase errors and coaxial cable lengths with a view to also identify water affected or faulty cables. A lack of correlation in this promising technique is attributed primarily to the temporal delay between the respective data sets compared.

While water ingress into the underground cable sections is responsible for the majority of identified faults currently within the antenna array, its prevalence as a fault source is attributed to being an artifact of the 1992/94 upgrade. It is surmised that once the water is eradicated using established techniques, the number of cables re-affected by water will be significantly lower than the current survey details. This can be confirmed by a repetition of techniques outlined in the current survey.

This result has important implications for the continued use of the array. It appears that numerous hardware revisions implemented in the previous antenna array upgrade have significantly addressed many of the array deficiencies, which significantly reduces the array maintenance required in the future. However, the expected natural attrition of array components together with the previously outlined concerns will demand that regular maintenance is performed and those noted problems areas are targeted. In particular, a strategy for dealing with the increasing number of more serious cable faults needs to be implemented. Suggestions for effective techniques in this area have been outlined.

Due to the size of the Buckland Park array (and hence the number of individual components that compose it) and its three decades of near continual use, valuable information on the progression of ageing array components has been obtained in this current and previous surveys. This is useful in applying both to future radar antenna array designs and to similarly long established radar installations. Cable-Balun-Antenna systems should have a straightforward design that maintains the integrity of each individual component used, with attention directed to not implementing that component outside of its specification. In terms of ageing arrays this design edict should be followed for any array upgrades as well.

With the now routine use of two transmitter chassis and the availability of a third, higher power transmitter chassis, there is an ever present demand for the complete antenna array to be fully operational at any one time. This Chapter has detailed various approaches to achieve this end.

3.6 Future work

Due to the versatility of the time domain reflectometry technique, it is most efficiently implemented with specific objectives in mind. This has been the approach used in the TDR techniques outlined in the previous sections and is useful in guiding future TDR

and maintenance work on the MF antenna array at the Buckland Park research facility. In the following section, procedural techniques to be implemented immediately alongside any TDR maintenance work using the current or similarly specified equipment are detailed. Areas mentioned involve tests to be completed pre-TDR work, more effective maintenance procedures and general equipment considerations. Tailoring equipment capabilities to future array maintenance needs sees the description of a third generation TDR equipment system for use in either general array documentation or detailed fault location investigation. While the upgrade of 1992/94 addressed some infra-structural needs of the array, the continued 24 hr use of the array 30 years after its installation sees the need for addressing the ageing and replacement issues of certain array components. Projections of likely component failure mechanisms are outlined and possible solutions noted.

The implementation of regular monitoring of the number of phase zero cycle steps required to phase calibrate each transmitter channel would assist in identifying malfunctioning CBA sub-systems. This could be easily implemented as a routine analysis module in the current system configuration with display focused on highlighting abnormal phase steps over time. Similarly, enabling the logging of the PA fault status of each transmitter channel offers another data input related to the current state of CBA sub-systems. While any anomalies detected in these parameters may not directly translate to faults within the CBA sub-systems they nevertheless provide valuable evidence for assessment in conjunction with other information. If implemented, both method results could be monitored remotely.

Any significant period of array maintenance should commence with the determination of system phase error values of the complete array. This will highlight any CBA sub-systems that require further investigation in identifying the cause of these abnormal values. Similarly, those antennas with relative phase errors exceeding -20° may indicate water ingress has occurred. The collection of any future phase error value data sets affords the opportunity to conclusively validate this technique. In

order to classify any CBA sub-system as operational it is imperative to complete a TDR probing of the system at the completion of maintenance procedures. Failure to use an adequate resolution TDR system as a confirmation tool on CBA sub-systems can lead to erroneously judging it as operational. Specific problems such as water ingress can be overlooked using only vector impedance metering confirmation techniques. Similarly, if compressed air is used to flush an air-cored dielectric of water, TDR techniques must be used to confirm all liquid has been expelled from the cable section and not re-located along the cable section. This is of particular concern with high nominal wavelength sections. The calculation of cable theoretical length can also be used in this regard, with any TDR derived cable electrical length diverging from expected cable length indicating insufficient water expulsion (sans other discontinuities). Such practices are also secondarily useful in monitoring the effectiveness of the air-compressor and moisture filter components of the compressed air system which degrade with continual use. Upon reconnecting cable sections after compressed air treatment it is necessary to ensure the Aeraxial-to-RG-11/U cable connection at the pole base is adequately re-sealed and offers no opportunity for further water ingress.

Noise present in TDR traces of a Cable-Balun-Antenna sub-system is mostly attributed to the signal from the connected dipole. This noise makes parameter estimation difficult. Controlling the noise at the source involves terminating the balun output with dummy load equivalent to the nominal dipole impedance. This is a time consuming task in order to facilitate a routinely brief check on a CBA sub-system. It is perhaps more useful to explore an alternative software or hardware solution. As mentioned before a significant increase in the number of waveforms that are averaged for each individual TDR trace will help contain this type of noise. Alternatively a low pass filter implemented in software or hardware could reduce the effect of the signal detected at the dipole if designed to block a suitable bandwidth centered at the dipole's resonant frequency of 1.98 MHz. Note however that as lower risetime pulses are used in the TDR system to increase system resolution more bandwidth along the

transmission line is required. This means that a filter of this type may affect the transmitted or received TDR pulse and allowances for this should be made. A filter design that may have less impact on the transmitted pulse is described by *Hewlett-Packard* [1965].

To further aid in cable maintenance, higher resolution TDR systems can be used to plot the beginning and end position of water along a cable section. This can then be correlated with information from adjacent cables to determine if cables sections contained in the same cable trench have been breached at a common location. This information can markedly reduce the amount of time spent on cable fault repair in the field as multiple faults spanning a number of cables can be addressed together.

An alternative to using compressed air as the gas used to force water from the underground cable sections is using compressed Nitrogen, which because of its strong triple covalent bond is an unreactive element. It is noted [*Straw*, 1994] that the low loss attributes of air-insulated coaxial cable depends partly on the air being kept dry in the dielectric cavity and that strictly speaking, air tight seals must be used at every termination. Keeping the air dry would also assist in limiting condensation problems but it is envisaged that any benefit of using compressed Nitrogen would be momentary because of the lack of an air-tight system in this cable network. More importantly the use of compressed Nitrogen is markedly less cost effective than compressed air and considering the minor nature of the condensation problem, its use is not warranted.

The optimization of CBA sub-systems will first involve the elimination of faults (cable, connector, dipole etc.) and progress to the tuning of the balun. To achieve effective fault elimination along a cable it is important to ascertain the nature of the faults that exist along the cable before the best method is determined for cable work. The precise nature of the fault determines the appropriate response from a range of possible solutions. For instance, the fault may be only a sheath deterioration causing a minor electrical discontinuity, perhaps via the corrosive effect of water contact on the outer braid. If this is the case the sheath could be cleaned of corrosion via a chemical treatment, the sheath mechanically repaired and heat shrunk to seal and protect the

outer braid. A minor, localized, variation in cable specification at this point may result but cable integrity has not been breached by the use of a connector or short replacement cable section, which may facilitate water ingress, and cable performance should not be significantly altered. This is the best case scenario. If the nature of the fault is more severe, such as a break penetrating to the air-cored dielectric or inner conductor by vermin activity or similar, all efforts should be made to repair the break in order to maintain performance and the ability to use the maintenance technique of compressed air on the air-cored dielectric for water eradication. If this can't be achieved then perhaps a connector or small section of surplus Aeraxial could be inserted (heat shrunk or alternatively sealed at the insertion points). Note that water eradication via compressed air can then be completed on the smaller, intact, sections of cable. While increasing the maintenance time required there are few alternatives to this arrangement.

It is apparent that regular array maintenance is essential in maintaining the array at peak operational status. Scheduled, short cycles of systematic maintenance could be applied to sections of the array or individual CBA sub-systems according to the demand. This approach minimises extended periods of radar down-time and reduces the number of CBA sub-systems to be examined within any one period during these short maintenance cycles. An approach such as this also allows labour and available equipment to be more effectively directed as requirements can be continually revised without significantly effecting radar operational status.

Commensurate with regular array maintenance is scheduled array monitoring. Weekly monitoring of CBA sub-system complex impedance provides a regular sample of overall array behaviour and documentation of impedance values allows realistic performance parameters to be established and achieved. In fact, documentation of the results of all maintenance work carried out on individual CBA sub-systems is vital for fault tracking over extended time periods. Only over extended time periods can the effectiveness of fault solutions be conclusively evaluated, particularly if environmental conditions have a significant part to play, as is the case for the Buckland Park field site.

An ordered, central repository for all CBA documents has been established in the MF CBA Database (MF CBAD), that allows easy access to individual CBA sub-system history primarily for assistance in periodic maintenance but equally useful for array surveys such as that outlined in 3.3.2. Similarly, maintenance procedures employed on components throughout the antenna array and radar system maintenance cycles have been documented [*Woithe & Grant*, 1999], and are being added to, in order to standardise and maintain the quality of maintenance carried out on the complete radar system.

The implementation of the more effective balun tuning technique described in section 3.4 will result in more power being radiated through the dipoles on average over a 12 month period. As mentioned before, the impedance variations of a dipole should be monitored over a 12 month period to ascertain the likely impedance variations under seasonal conditions. This will provide average impedance information that could be utilised in any dummy dipole load used in balun tuning procedures thereafter. Any monitoring of a test dipole could include data output from the Automatic Weather Station (AWS) located at the Buckland Park field site adjacent to the MF antenna array. This could provide valuable atmospheric parameters at surface level for later correlation with antenna impedance. At the same time, soil conductivity and water content could also be recorded (employing modified TDR techniques, refer to *Davis & Annan* [1977] and *Dalton et al.* [1984] or by using Frequency Domain Reflectometry (FDR), refer to *Friel & Or* [1999]), as these parameters have a marked effect on dipole characteristics. Upon successful tuning, the baluns operation could be tested using equipment similar to a TDR configuration but providing device under test interrogation at 1.98 and 5.94 MHz. This will allow an immediate confirmation of successful balun tuning.

It is envisaged that future maintenance of the Buckland Park site will require a high resolution system that can be used for both general CBA sub-system monitoring (fault notification/specification confirmation/length calculation) and also the more

detailed fault location (fault location coupled with a cable locator) in the field. Because of the extensive network of cables (∼70 km) and age of the array, commercially available TDR systems/network analysers[15] and cable locators may be a cost effective solution. Such TDR systems are often ruggedly constructed for field work and include most readily needed functions in a single unit. Alternatively, because traditional commercially available TDR systems up until recently comprise a simple arrangement of a pulse generator mated to an oscilloscope, an equivalent system could be configured from pre-existing equipment (i.e. a system similar to those already described in section 3.2.1 and section 3.2.2). While commercial, state-of-the-art, TDR systems centre around this basic configuration, many current products now incorporate more complex networking options and capabilities that are difficult to emulate when assembling individual components.

In order to detail the specific requirements of a third generation TDR system it is thought more appropriate to describe a component assembled system as opposed to available commercial systems because such a description can serve as a minimum specification for a commercial system in any case, if that approach was later deemed more appropriate. Such a system is described in the following paragraphs.

A third generation TDR system (designated equipment system III) would be capable of operation in two distinct modes. The first mode (TDR fault location) facilitates traditional TDR capabilities (employing the Pulse/Impulse or Step-Voltage technique where necessary), and allows the integrity of the device under test to be examined with emphasis on water ingress, cable fault and cable length measurements. The use of up-specified system components in an arrangement similar to the two currently employed test systems would be applied only on the cable section of interest and would omit all other connected cable sections. The ability to tailor the chosen TDR technique (Pulse/Impulse or Step-Voltage) allows more flexibility in approaching and solving cable faults, where the Step-Voltage technique is perhaps better applied to short cable

[15]Network analysers are Frequency Domain Reflectometry (FDR) devices. They typically generate and measure sinusoidal voltages and currents over a broad frequency range, but can display information in a TDR type format via an inverse fast Fourier Transform [*Hewlett-Packard*, 1998].

lengths with impedance problems and the Pulse/Impulse technique is more appropriate for longer cable sections.

A second mode (CBA performance) of this third generation system would allow probing of the complete CBA sub-system at its operating frequency of 1.98 and 5.94 MHz. Here, a Gaussian pulse characteristic of that generated by the radar, is applied to the CBA sub-system in order to simulate realistic operational performance levels. Thus pertinent CBA sub-system characteristics such as cable attenuation, VSWR etc. can be estimated. This would be achieved using a capable pulse generator or a pulse generator coupled with a function generator, with display via a digital storage oscilloscope. Switching of the baluns for 1.98 or 5.94 MHz operation would be performed via a suitably rated DC power supply. Both modes of operation would display and archive results using a laptop computer, with a printer providing hardcopy facilities. The Figure 3.26 displays a block diagram of this system with the upper diagram showing Mode One application and the lower Mode Two. Mode one, used for measurement of cable parameters, will aim for a system that adheres to having a system risetime ten times better than the system being tested [*Botos*, 1968]. As mentioned previously, lowering system risetime can be achieved by selection of capable (low risetime) equipment and the arrangement of said equipment. For accurate TDR location applications a pulse risetime of the order of 100 ps is desirable. It is expected that all signal monitoring may be accomplished using a more commonly available Digital Storage Oscilloscope (DSO) but may require the use of the sampling technique (e.g. *Hewlett-Packard* [1965]; *Grivet* [1970]) incorporated into the current Digital *Sampling* Oscilloscopes (DSpO) [*Agilent*, 2001*b*]. This is because the faster risetime pulses (e.g. 100 ps) contain frequencies up to 10 GHz and in order to avoid aliasing when reconstructed they need to be sampled at a minimum of twice as fast as the signals highest frequency component. Only the architecture of Digital Sampling Oscilloscopes can facilitate these high sampling rates. A disadvantage of the Digital Sampling Oscilloscopes is that they have a limited input dynamic range of about 1 V peak-to-peak. However the sampling capabilities and digital filtering available via these oscilloscopes

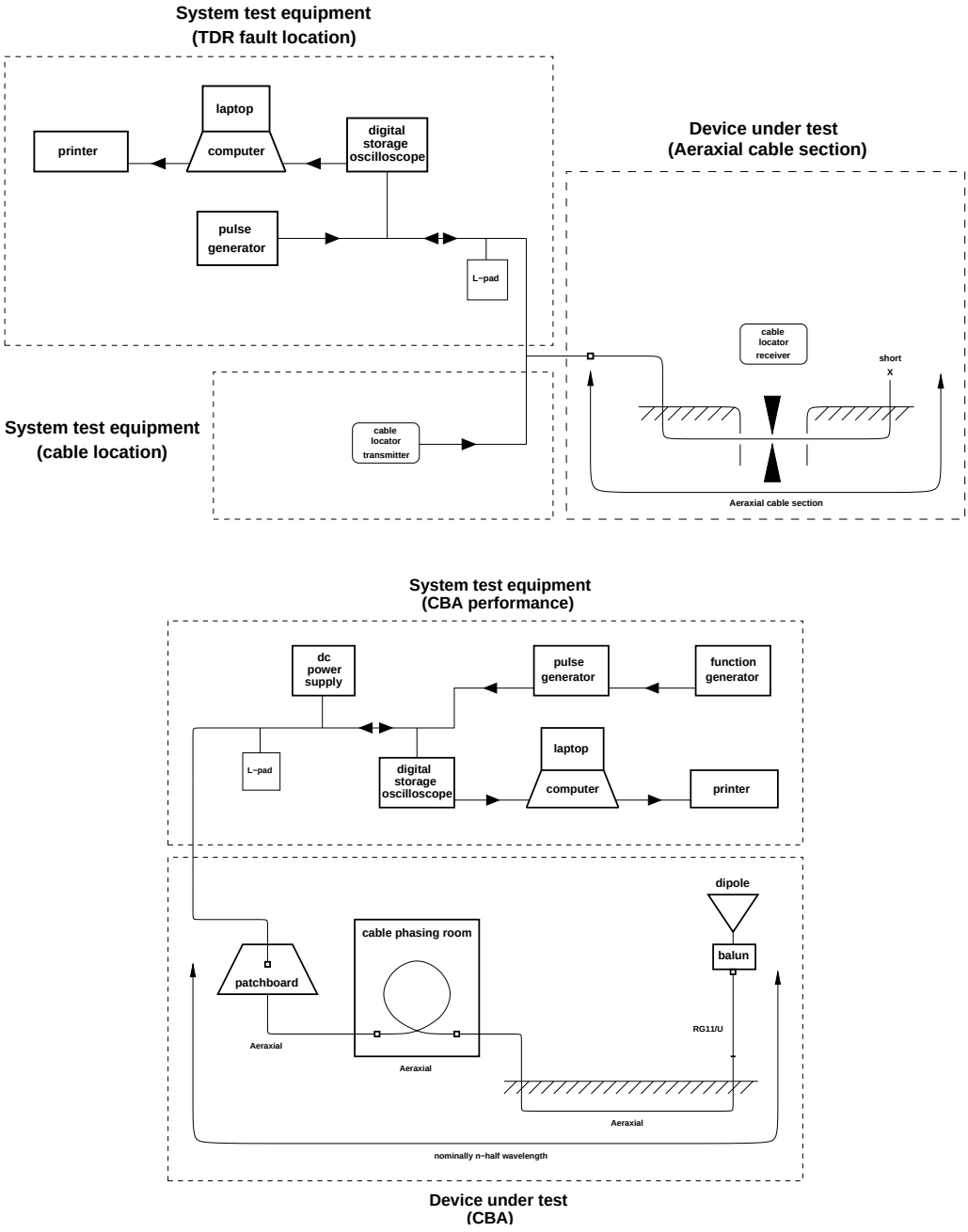

Figure 3.26: Equipment system III block diagram.

can contribute significantly to noise reduction etc. Again, a laptop computer or PC allows convenient TDR trace manipulation and storage.

A pulse generator circuit design for Mode One operation could developed from that outlined by *Straw* [1994], *King* [1989] or *Englund* [1998]. However, the generation of the fastest risetimes in the sub-nanosecond range (∼100 ps) are often obtained using the abnormal (avalanche breakdown) mode of a transistor or via tunnel

diode sources [*Editorial*, 1974]. While offering excellent risetime capabilities, tunnel diode sources applied in TDR environments are not without their drawbacks (e.g. *Cole* [1977]; *Editorial* [1974]), most notably their limited amplitude output of 250 mV to 500 mV, depending on the backmatching of this source. In the current TDR system configuration this would require exceptional signal processing to obtain adequate pulse return information in the presence of system noise. This situation may be improved by the replacement of the dipole under test with a dummy load of equivalent value but it is thought that the length of the cable section under test and its inherent cable attenuation characteristics will still limit return pulse amplitude to an unacceptably low level. If these considerations are addressed and a risetime of 300 ps is acceptable, *Andrews* [1970] describes a simple circuit that addresses other minor tunnel-diode implementation drawbacks. Alternatively, current commercially available systems offer 45 ps risetimes with a 10 V step [*Andrews*, 1989]. It should be noted that at very low pulse risetimes ($\leq$ 50 ps) there can be a change in the mode of propagation should the pulse contain frequencies whose electrical quarter wavelength is approximately equal to the cable outer conductor inner diameter [*Strickland et al.*, 1970]. This situation should be avoided in TDR systems because some energy of the original TEM (Transverse Electric Magnetic) mode is converted to the TE_{11} mode at each discontinuity and it is advisable that all energy remain in the TEM mode throughout TDR system propagation.

The impedance matching of all system devices is important. Properly matched components eliminate unwanted reflections and allow more accurate amplitude measurements to be be made. This facilitates the calculation of many coaxial cable parameters pertinent to evaluation of performance in the field. Here, the primary concern is transforming the 50 Ω impedance of most test equipment components to the nominal 70 to 75 Ω of the Aeraxial coaxial cable. This is achieved by the insertion of suitable resistor values between cable section input and DSO input. *Hewlett-Packard* [1965] describe a simple matching L-pad for this purpose. If the characteristic impedance of the coaxial line to be matched is $>$ 50 Ω then the resistance in series with Z_O, R_1

$= \sqrt{Z_O(Z_O - 50)}$ and shunt resistance, $R_2 = 50\ Z_O\ /\ R_1$. The case for matching an equipment system of a nominal 50 Ω to that of the 75 Ω Aeraxial coaxial cable using this L-pad is shown in Figure 3.27. Some attenuation of the transmitted signal will occur with this arrangement however.

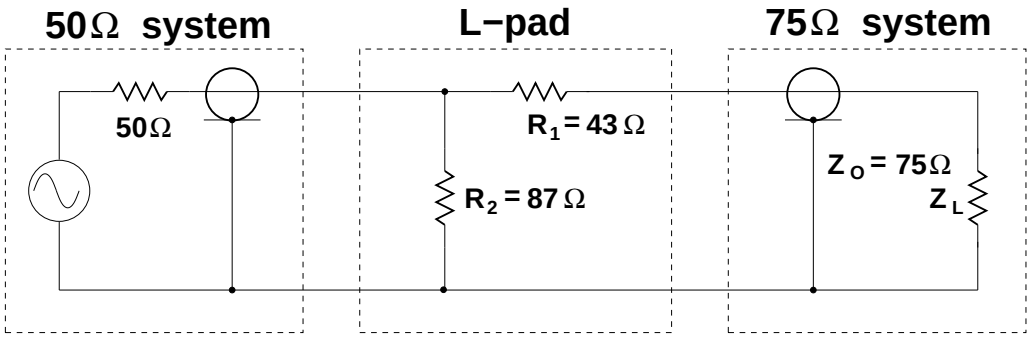

Figure 3.27: L-pad for matching a 50 Ω source impedance to a 75 Ω Aeraxial coaxial cable (after *Hewlett-Packard* [1965]).

The ability to operate a system such as equipment system III in Mode One from the DC power source of a vehicle battery is considered desirable. This allows flexibility in test equipment connection and may suit situations where the fault lies in close proximity to the balun/dipole. This configuration has advantages in that less degradation of the pulse risetime may occur, resulting in a more accurate fault location being calculated as well as the simplified measurement of cable distance to a fault when eliminating any above/below ground cable transitions.

It is expected that even with an increase in test equipment resolution, the location of cable faults will require the selected use of more active TDR fault location techniques. This is in contrast to the passive fault location techniques described and used previously. This approach is envisaged due partly to the often encountered lack of visible damage at known fault sites and the extended time required to isolate such a fault that is characteristic of a passive approach. A benefit of active TDR fault location is that immediate feedback on the success or failure of fault location is obtained at the risk of possible permanent damage to the coaxial cable under test. The damage of a previously fully functional section of cable is to be avoided and in order to minimize

the risk of this outcome, less intrusive active techniques should be used. A typical process (outlined in e.g. *Tektronix* [1965]) is described as follows where, to locate the position of a small, short-duration discontinuity, a second small discontinuity can be added near the original. This can be achieved by clamping pliers or drilling a small hole in the outer wall of the coaxial cable. This can induce a shunt capacitance, which if located at the precise fault location can produce a reflection of opposite polarity to the original fault. The result is a minimal or much reduced total reflection at the fault location, confirming the exact fault location. If the positioning of the second discontinuity is less successful, the subsequent re-application of this technique can be directed via the TDR trace to obtain an exact location. A further consideration in the effective application of this technique is the requirement for two people to execute this technique with the extensive use of voice radio communication. Unfortunately this technique relies heavily on a trial and error process which is to be avoided in the presence of more efficient techniques. However in the absence of significant increases in system resolution this process may yield success.

A consistent and comprehensive labelling system of all buried cable bundles needs to be implemented as new bundles are located with any cable location equipment. This will allow a significant reduction in labour time used in isolating the physical location of a specific underground coaxial cable for repair. It is suggested that coloured plastic surveyors markers could be used for this purpose with cable depth inscriptions. These highly visible markers will not hinder vehicular activity over the array diameter.

Any new cable laid can be measure with this third generation system and an *ideal* or *at installation* TDR trace recorded for future reference of original cable performance. This also allows confirmation that the cable is defect free and adheres to the required cable specification. In fact at the time of writing new cable lengths have replaced the original 6E5 & 6N5 cable sections. Physical cable length was measured accurately before burial and could be used in the future for VF calculation or cable property testing.

The installation of multiple antenna phasing cables is an ideal application of Differential TDR techniques [*Hewlett-Packard*, 1965]. Here two coaxial cables can be paralleled with the reflections from the end of the cables appearing on one trace. Assuming one cable has been properly phased (e.g. an existing cable of the desired electrical length), trimming the non-phased cable of successive lengths until the cable end returns are superimposed will achieve matching phased cables. The degree to which this can be achieved depends on the resolution of the system.

Presently, any array maintenance cycle consists of three major parts. First an assessment is made of what CBA sub-systems require attention. Secondly, those CBA sub-systems are investigated and repaired, with the third maintenance component being a confirmation that those antennas are performing as expected. These tasks are complicated by the sheer physical size of the array, the relatively remote location of the site and the requirement for suspension of radar observations. Future array maintenance, in terms of labour cost and time spent, could benefit from the automation of appropriate parts of the current maintenance cycle. It is envisaged that the initial assessment and final confirmation of the antenna maintenance cycle could be completed by an automated system and that only the fault rectification work on site require manual intervention. Further, this automated system could be used periodically (e.g. at the start of a radar acquisition period) to provide regular data on the current state of the antenna array. This automated system could also assist in the manual element of array maintenance. Here, the automated system could be manually controlled to inspect individual CBA sub-systems in an effort to isolate faults, in a similar manner to the employment of equipment system I & II. This information can then be used for location and repair work in the field. A suggested configuration of an automated system is outlined in Appendix F.

With the implementation of an effective maintenance regime it is expected that the MF antenna array could achieve full operational status for at least the next decade using the majority of the current infrastructure. This projection is based on the current evidence that suggests that most current water affected cables have been permanently

fixed and most cable faults are of a manageable level. Further water ingress throughout the array is thought to be sporadic in geographic terms, aside from a small clustering of occurrence associated with local water courses, but is generally of a manageable level. However, some CBA sub-systems will require extensive maintenance work in the near future and the question of wholesale replacement of these cable sections arises. Indeed, as mentioned above, at the time of writing the complete cable sections of 6E5 & 6N5 have been replaced with an equivalent cable type in the same configuration as the existing CBA sub-systems. Is this the most appropriate upgrade path for the Buckland Park MF array?

Any assessment of future upgrade pathways must consider two main criteria. Firstly the projected use of the array will establish what future capabilities the array must provide for. Secondly, the most successful upgrade pathway will address all currently encountered array design problems. In addressing the first criterion, it is assumed that future use of the array will continue the lineage of the past three decades of use, in that a high degree of configuration flexibility will be demanded, both in terms of atmospheric phenomena to be investigated and how that phenomena is to be studied. The results of this Chapter contribute to satisfying the second criterion, with continued array monitoring further focusing attention on those areas of array design in need of attention. In establishing these two main criteria, possible upgrade pathways are briefly discussed in the following paragraphs.

In order to simplify and increase the effectiveness of maintenance of the array *Ludborzs* [1996] outlines a modular cable replacement system. Rather than using a single continuous cable section from cable room to balun, each pole base has a junction box with short buried cable sections connecting between each junction box. Thus any single connection to a balun/dipole comprises multiple short cable sections. The multiple wavelength requirement for each complete CBA sub-system is preserved by using phase delay units where necessary. Benefits of this system are that smaller sections of damaged cable may be more easily replaced and the exclusion of water is better facilitated by shorter cable lengths. Disadvantages of this system are that

a significant increase in complexity is attained as well as an increase in the number of connections required in the field. Increasing electronic complexity in the midst of harsh environmental conditions tends to lead to an increase in maintenance problems. Also, multiple connections on a single cable section impart losses that can be best minimised with single, longer cable sections.

Alternatively the original single cable sections could be preserved but groups of cables could be housed in buried [*Baggaley & Galligan*, 2001] or surface laid conduit. Plastic conduit [*Schetgen*, 1994] or flexible irrigation hose could be used, employing waterproof seals where single cable sections emerge from the multi-core arrangement near each antenna pole. This has been previously implemented with success (e.g. *Gamble* [1997]). Advantages of this arrangement are that the cable is protected from the environmental conditions as well as vermin activity. Also, less robust coaxial cable (in terms of its ability to be buried etc.) may be used, as parts of the cable jacket's function is now afforded by the conduit. A core disadvantage of this approach is the difficulty in accessing faults mid-conduit for maintenance. Also, if the conduit was not buried, vehicular access to the array would be limited which is important not only for array maintenance purposes but for general infrastructure maintenance such as limiting grass height to reduce fire hazards.

As detailed in the previous sections it appears that many of the design faults of the original antenna array system have been addressed in the upgrade of 1992/94. Further, the basic layout of the cable system has presented no major flaws aside from the difficulty in accessing the underground cable for maintenance and its development of cable faults in the ensuing years. Perhaps further refinement of the existing sound array design presents the most effective (in terms of cost and design) upgrade path.

The projected failures of the cable sections include Aeraxial section outer sheath breaches instigated by weathering or vermin activity, together with low level water ingress into the air-cored dielectric primarily arising from moisture/vapour penetration and said outer sheath breaches. These problems can be addressed to a large extent with current technology coaxial cable.

The Aeraxial cable currently in use was chosen for its ability to be buried and the cable jacket has provided good protection considering the extended years of use. However jacket brittleness, resulting partly from years of burial, has been observed. In addition to the mechanisms outlined above, general coaxial cable failures are primarily caused by effects of ultra-violet exposure, high humidity, galvanic action, salt-water and corrosive vapours on the materials used [*Times Microwave Systems*, 2002].

Assuming that one coaxial cable type will be used from patchboard to balun, it will have some exposure to damaging ultra-violet light and thus require some degree of protection. Here polyethylene compounds offer increased longevity over standard polyvinyl chloride (PVC) type cable jackets. Connectors and pin-holes in the jacket offer entry points for water vapour, rainwater, salt water and corrosive vapours. In fact all materials exhibit a finite vapour transmission rate indicating that it is difficult to exclude all vapours from a cable over time and some degree of vapour intrusion will inevitably occur. Coaxial cables that offer high resistance to these factors may incorporate a number of technologies. These include (e.g. *Belden* [1993]; *Times Microwave Systems* [2002]); water proof connectors incorporating O-ring seals together with externally sealing around all connections in-place to prevent moisture entry at physical cable breaks; voids within the coaxial cable could be filled with moisture proofing compounds that don't harden with age; jackets can be fashioned such that they are pin-hole free, the use of the least porous thermoplastics such as FEP (Fluorinated Ethylene Propylene) can be used; tape bonded to the cable jacket can prevent interference between the jacket and the shield from becoming a moisture path and incorporating various forms of armour tape (metallic or nylon) to the jacket or outer sheath offers protection against vermin activity that if not applied can negate the protection afforded by all previous forms of cable protection. Any material used for armouring a cable must have corrosion resistance as it will be exposed to the environment after attack. It has been reported [*Hughes*, 1997] that cables having diameters > 50 mm are safe from gnawing as this diameter is larger than the open jaw of the offending vermin. Unfortunately a diameter of this size is generally unsuitable in this

application.

Once installed, cable performance should be monitored at least every two years [*Straw*, 1994], including visual and TDR assessment, with cable replacement recommended when losses exceed 1 dB. Recommended procedures for burying the selected cable type suggest laying 150 mm thickness of sifted soil, which primarily stops damage to the cable sheath by stones, on the bottom of a trench whose total depth is based on future disturbance by land use [*Hughes*, 1997]. A similar thickness of sifted soil is layered on top of the cable.

Regardless of upgrade path chosen, the testing of any prototype system is vital due to the required implementation on the scale of the existing array. As individual CBA sub-systems require replacement, prototype systems could be installed and monitored to ascertain solutions to any unanswered questions.